Charles University
Faculty of Science

Study programme: Reproduction and Developmental Biology

Bc. Vendula Václavková

Působení laminu A/C na DNA demetylaci paternálního prvojádra

Influence of lamin A/C on paternal pronucleus DNA demethylation

Diploma thesis

Supervisor: Mgr. Helena Fulková, Ph.D.

Praha, 2022

Prohlášení:

Prohlašuji, že jsem závěrečnou práci zpracovala samostatně a že jsem uvedla všechny použité informační zdroje a literaturu. Tato práce ani její podstatná část nebyla předložena k získání jiného nebo stejného akademického titulu.

V Praze, 21. 04. 2022

Podpis

Poděkování:

V první řadě bych ráda poděkovala své školitelce Mgr. Heleně Fulkové, Ph.D. za přijetí do jejího týmu, sdílení odborných zkušeností a zejména skvělé vedení diplomové práce. Také bych ráda poděkovala Jasper Chrysolite Paul, MSc. za pomoc s technickými obtížemi při práci v laboratoři. Dále bych ráda poděkovala Bc. Zuzaně Smékalové za pomoc při dokončení mé práce a take Mgr. Petře Herlové za psychickou podporu při práci. Na závěr děkuji své rodině, příteli a přátelům za ohromnou podporu a povzbuzení při psaní této práce.

Abstrakt

Po oplození dochází k řadě dynamických epigenetických změn, které přestavují genom gamet a zajišťují totipotenci zygoty. Procesy je možné pozorovat v obou rodičovských prvojádrech, avšak aparát zajišťující epigenetickou dynamiku se pravděpodobně nachází v mateřském oocytu, konkrétně v jeho zárodečném váčku (germinal vesicle GV).

GV je možné rozdělit na dvě frakce: solubilní a nesolubilní. Pravděpodobnou schopností solubilní frakce je remodelace hlavičky spermie a zajištěné vznik otcovského prvojádra, zatímco na reprogramování otcovského genomu a zajištění vývojové competence by se mohla podílet nesolubilní frakce.

Tato práce se věnovala jedné z epigenetických modifikací a to DNA metylaci, respektive její rychlé ztrátě po oplození. Jedna z možností, jak k tomuto ději může dojít, je oxidace metylovaných bazí a jejich následná oprava a záměna pomocí opravného mechanismu base excision repair (BER).

V této práci jsme testovali, zda protein lamin A/C, součást nesolubilní frakce, je možným kandidátem, který může zahájit aktivní demetylaci DNA prostřednictvím BER. Pro práci bylo potřeba připravit takové GV oocyty, které by obsahovali jak solubilní část GV, tak protein lamin A/C. K získání cytoplastů obsahujících solubilní frakci GV byla použita metoda selektivní enukleace. Tyto cytoplasty byly oplozeny *in vitro* a byl analyzován epigenetický stav vzniklých prvojader. Ke zjištění metylace DNA konkrétních sekvencí byla použita metoda bisulfitová sekvenace.

Výsledky práce nepotvrdily roli laminu A/C v demetylaci DNA po oplození. Nicméně, obecně role nesolubilní složky GV nebyla vyloučena. Tyto výsledky společně ukazují, že změny metylace DNA po oplození jsou komplikovaný a mnohočetný proces a další komplexnější pokusy by měly být předmětem dalších studií.

Klíčová slova: aktivní demetylace, zárodečný váček, lamin A/C, base excision repair (BER)

Abstract

A series of dynamic epigenetic changes need to happen to rebuild the gamete's genome after fertilization and to secure the totipotency of the zygote. The processes can be observed in both parental pronuclei, although the machinery providing the epigenetic dynamics probably lies in the maternal oocyte, more specifically in the germinal vesicle (GV).

GV can be divided into two fractions: a soluble and an insoluble fraction. The probable ability of the soluble fraction is remodelling the sperm head and the paternal pronucleus formation, while the insoluble fraction could be involved in reprogramming of the paternal genome and ensuring the developmental competence.

This thesis was focused on one of the epigenetic regulations which was DNA methylation and its rapid loss after fertilization. Putative mechanisms, which can occur there are the oxidation of methylated bases and their subsequent repair and replacement through the base excision repair (BER). This thesis tested a hypothesis that a protein lamin A/C, found in the insoluble fraction of the GV, is a possible candidate participating in the active demethylation through BER.

To examine the role of lamin A/C in BER, it was required to prepare such GV oocytes, which would contain both the soluble part of GV and protein lamin A / C. The selective enucleation was used to obtain cytoplasts containing the soluble GV fraction. These cytoplasts were then fertilised *in vitro* and the epigenetic status of the formed pronuclei was analysed by bisulfite sequencing to examine the methylation status of specific sequences.

This thesis did not confirm the hypothesis that lamin A/C participates in the DNA demethylation after fertilization. However, the role of the insoluble GV fraction has not been excluded. These results together provide an insight into DNA methylation reprogramming after fertilization and suggest its systemic complexity and it should be the subject of further studies.

Key words: active demethylation, germinal vesicle, lamin A/C, base excision repair (BER)

Abbreviations

5caC	5-carboxycytosine
5fC	5-formylcytoine
5hmC	5-hydroxymethylcytosine
5mC	5-methylcytosine
AID	Activation-induced deaminase
AP	Apurinic/apyrimidinic site
APOBEC1	Apolipoprotein B mRNA editing enzyme catalytic polypeptide 1
BER	Base excision repair
C	Cytosine
$CaCl_2$ x 2 H_2O	Calcium chloride dihydrate
CE	Complete enucleation
CGI	CpG island
COCs	Cumulus-oocyte-complexes
CpG	Cytosine-phosphate-guanine dinucleotide
DNA	Deoxyribonucleic acid
DNMT1/3a/3b/3L	DNA methyltransferase 1/3a/3b/3L
DPPA3	Developmental pluripotency-associated protein 3
DSB	Double strand break
DSBH	Cys-rich domain and a double-stranded β helix
EDTA	Ethylenediaminetetraacetic acid
EtOH	Ethanol
G	Guanine
GSE	Gonad-specific expression gene
GSH	Reduced glutathione
GV	Germinal vesicle
GVBD	Germinal vesicle breakdown
hCG	Human chorionic gonadotropin
HR	Homologous recombination
HS	Heparan sulfate
HTF	Human tubal fluid medium
IBMX	Isobutyl-methylxanthine

JBP	J-binding protein
KCl	Potassium chloride
KH_2PO_4	Potassium phosphate
LADs	Lamina-Associated Domains
LINE-1	Long interspersed nuclear elements
MBCD	Methyl-β-cyclodextrin
MBD4	Methyl-CpG-binding domain protein 4
MetOH	Methanol
$MgCl_2$	Magnesium chloride
$MgSO_4$ x 7 H_2O	Magnesium sulfate heptahydrate
MII	Metaphase II arrest
MPF	Maturation promoting factor
Na_2HPO_4	Disodium hydrogen phosphate
NaCl	Sodium chloride
$NaHCO_3$	Sodium bicarbonate
NaOAc	Sodium acetate
NaOH	Sodium hydroxide
NHEJ	Non-homologous end-joining
NL	Nuclear lamina
NM	Nuclear membrane
Oct-4	Octamer-binding transcription factor 4
PBS	Phosphate-buffered saline
PCR	Polymerase chain reaction
PGCs	Primordial germ cells
PMSG	Pregnant mare's serum gonadotropin
PN	Pronucleus
PVA	Polyvinyl alcohol
PVDF	Polyvinylidene difluoride
RIPA	Radioimmunoprecipitation assay buffer
ROS	Reactive oxygen species
SAM	S-adenosylmethionine
SCD	Sperm chromatin decondensation
SDS-PAGE	Sodium dodecyl sulfate–polyacrylamide gel electrophoresis

SE	Selective enucleation
SMUG1	Single-strand-selective monofunctional uracil DNA glycosylase 1
STPG4	Sperm-Tail PG-Rich Repeat Containing 4
T	Thymine
TBS	Tris buffered saline
TBST	TBS with Tween
TDG	Thymine DNA glycosylase
TEMED	N,N,N´,N´-tetramethyl-ethylenediamine
TET1/2/3	Ten-eleven translocation1/2/3
TYH	Toyoda, Yokoyama, Hoshi medium
U	Uracil
WB	Western blot

Contents

1 Introduction

Fertilization occurs at the very beginning of the development of many living organisms. During this process, two unique types of cells, the sperm and the egg, combine to form a zygote. While the sperm loses most of its cytoplasm during spermiogenesis, the egg is one of the largest cells and contains all the typical cellular organelles. Therefore, it is the egg that provides the building blocks for the early embryo. For the egg, the fertilization does not seemingly represent an evident cellular transformation. However, the egg must still complete the second meiotic division and its genome is substantially remodelled. Nevertheless, the genome remodelling of the sperm is much more evident (Gilbert, 2014).

The machinery for the post-fertilization male gamete remodelling and paternal pronucleus formation is located in the female egg. For this remodelling, the germinal vesicle (GV), i.e. the oocyte nucleus, is needed. Roughly divided, GV contains two fractions: insoluble (stably bound nuclear proteins, e.g. the nuclear envelope, or stably DNA-bound proteins) and soluble (soluble nuclear envelope components, nuclear bodies etc.) (Merriam & Hill, 1976). When the whole GV is removed from the oocyte, the sperm head is unable to form a functional pronucleus (Usui & Yanagimachi, 1976). When a somatic cell nucleus is transferred into such a cytoplast, its morphology does not change and as expected, it does not take up GV components (Ogushi et al., 2005). However, when the soluble fraction of GV is released into the cytoplast prior to enucleation, these components rapidly translocate into the somatic nucleus and lead to a partial remodelling in a replication-independent manner (Matoba & Zhang, 2018). However, functional studies show that unlike the somatic nucleus, the sperm does not form a fully functional one.

One of the processes which take place after fertilization is DNA demethylation (Suzuki & Bird, 2008). The post-fertilization demethylation can be divided into two processes: active DNA demethylation and replication-dependent passive DNA demethylation (Moore et al., 2013). These processes will be discussed in more detail below. The active demethylation is a rapid process, and it is completed prior to the first zygotic DNA replication. The DNA demethylation occurs in the whole genome but predominantly in the paternal pronucleus (Gu et al., 2011; Iqbal et al., 2011). The passive demethylation typically involves both parental genomes (Rougier et al., 1998). Finally, later during the lifetime, there is the second wave of genome-wide demethylation, which occurs during the primordial germ cell formation.

Although these processes likely have much in common, the exact mechanism of the post-fertilization DNA demethylation remains unknown. Several studies have proposed specific enzymes and mechanisms; however, the process of the post-fertilization demethylation has not yet been completely elucidated and remains a subject of intensive investigation.

2 Literary overview

2.1 Influence of oocyte on sperm after fertilization

To allow for the demethylation and other processes to take place, the embryos must form parental pronuclei. It is generally accepted that the building blocks originate from oocytes, and they are accumulated prior to fertilization, when, among other things, the maturation of the oocytes is completed. These factors are necessary not only for the completion of the oocyte maturation and the formation of female pronucleus but are also important for the sperm head remodelling and the functional male pronucleus formation. All these events are critical for one-cell embryo formation followed by activation of embryonic transcription of its genome (Perreault, 1992).

Oocyte factors are involved in numerous processes and many of them are not known to date. Factors important for the sperm transformation are the matter of an intensive research of the scientific community. One of the partly elucidated processes is sperm chromatin decondensation (SCD). It has been proposed that important factors required for SCD are present inside of the oocyte GV. To release these factors germinal vesicle breakdown (GVBD) needs to occur. Without the GVBD (Ogushi et al., 2005) or if the GV is removed (Usui & Yanagimachi, 1976), SCD does not take place. Another example of a maternal factor required for SCD is the growth arrest-specific gene 6 (Gas6). Gas6 is essential for biosynthesis of heparan sulfate (HS) and glutathione (GSH) (K. H. Kim et al., 2018). These molecules are required for sufficient cytoplasmic maturation, SCD and pronuclear (PN) formation after fertilization. In mammals, oocyte GSH reduces protamine disulfide bonds (Luberda, 2005), while HS is highly negatively charged and therefore is able to bind to protamine in mice and during SCD HS removes protamines from sperm DNA (Romanato et al., 2008).

Maternal factors have influence not only on the sperm remodelling and pronucleus formation, but also on the level of epigenetic reprogramming. One of the main changes of this kind is the sperm DNA demethylation.

2.2 Dynamics of DNA methylation

One of the epigenetic heritable modifications of DNA, next to the histone modification or RNA interference, is adding a methyl residue at the cytosine base, specifically at the 5C position, to create 5-methylcytosine (5mC). DNA methylation of the mammalian genome occurs in various biological contexts e.g., genomic imprinting, gene activation or silencing, X-inactivation etc. At the base level, 5mC can be found in different contexts along the DNA sequence, but mostly 5mC is associated with the guanine (G) base in the 3´position. Therefore, C and G together create cytosine-phosphate-guanine dinucleotide (CpG). CpGs often occur at the promoter site of genes. The presence of 5mC in such an instance might have an impact on the transcriptional activity of the specific promoter (Weber et al., 2007). Higher concentration of CpG dinucleotides with percentage greater than 50% in a sequence of 200 bp and with CpG frequency that is greater than 6% is called CpG islands (CGIs) (Gardiner-Garden & Frommer, 1987; Suzuki & Bird, 2008).

Depending on the sequence of the DNA, DNA methylation can be gained, lost, or maintained throughout life. The addition of the methyl group to C is catalysed by a protein family of DNA methyltransferases (DNMT) (Moore et al., 2013). These enzymes are able to transfer a methyl residue from S-adenosyl methionine (SAM) to the cytosine resulting in creation of 5mC (Martin & McMillan, 2002). There are three main members of this family: DNMT1, DNMT3a and DNMT3b. With respect to DNA, two modes of methylation are possible: the DNA methylation is either maintained or established *de novo*. The maintenance is ensured by DNMT1. DNA methylation typically occurs in a symmetric manner. This means that when a CpG dinucleotide is methylated, the corresponding CpG dinucleotide on the complementary strand is methylated as well. This pattern is temporarily lost during DNA replication. The maternal strand carries the original methylation pattern, while the nascent strand is unmethylated. This pattern of asymmetric methylation is also known as hemimethylation. In most cases, DNMT1 binds to the replication fork and methylates the newly synthesised strand copying the methylation pattern from the maternal strand (Hermann et al., 2004). On the

other hand, *de novo* methylation is carried out by DNMT3a and DNMT3b. These enzymes are able to methylate DNA with no need for hemimethylated DNA. *De novo* methylation occurs during embryogenesis and gametogenesis (Okano et al., 1999).

Introduction of the methyl groups to DNA is only one of the modes how DNA can be modified. However, DNA methylation can be lost as well. This process is called DNA demethylation. During the mammalian development, there are two major waves of genome-wide DNA demethylation: the first wave occurs right after the fertilization in the zygote (Santos et al., 2002), and the second wave occurs in the germline, and it is completed during later stages of germ cell development (Hajkova et al., 2002).

There are two modes of DNA demethylation: passive demethylation and active demethylation.

2.2.1 Passive demethylation

In theory, each DNA replication would lead to a 50% loss of DNA methylation because the nascent strand is not initially methylated during replication. To prevent this, DNMT1 ensures that DNA methylation is maintained. If DNMT1 is lacking or is dysfunctional, the methylation maintenance activity is lost. This leads to a decrease of methylation and the process is called passive demethylation or replication-dependent demethylation. Therefore, passive demethylation can occur in dividing cells (S. C. Wu & Zhang, 2010). It can also be observed after fertilization (Guo et al., 2014; Kohda & Ishino, 2013). This will be described in more detail in the next parts of the introduction.

2.2.2 Active DNA demethylation

It was originally thought that the methylation is an irreversible modification and can be decreased only through replication as mentioned above (Ramchandani et al., 1999). Nowadays, it is clear that DNA methylation is erased actively as well.

Several mechanisms can be considered for active demethylation. Perhaps the most intuitive reduction of DNA methylation is a simple removal of methyl residue from cytosine (Bhattacharya et al., 1999). However, another way of losing DNA methylation is through elimination of the whole 5mC typically through a DNA repair pathway (Gehring et al., 2009).

Finally, another mechanism which leads to erasure of methylation is changing the chemistry of 5mC by enzymatic activity to obtain different status of the cytosine base (Iyer et al., 2009; Morgan et al., 2004; G. L. Xu & Walsh, 2014).

The first mechanism, a direct removal of the methyl group from the 5 position of the cytosine seems to be quite improbable. The carbon-carbon bond is too strong to make it possible (Bochtler et al., 2017). Next, the removal of the whole 5mC, could be performed by a base excision repair (BER). However, other repair mechanisms can also play a role in DNA demethylation, e.g. nucleotide excision repair (Schuermann et al., 2016). The third possibility of active demethylation is linked to enzymatic activities such as the enzymatic oxidation provided by ten-eleven translocation (TET) enzymes (Gu et al., 2011). TET enzymes are a family of DNA dioxygenases, which are able to create 5-hydroxymethylcytosine (5hmC) from 5mC by oxidation. This may continue with oxidation of 5hmC to 5-formylcytosine (5fC) and 5-carboxycytosine (5caC) (Ito et al., 2011). The oxidation of 5mC can also lead to thymine generation. In this case, T-G mismatches are created, and thymine must be removed. This can be done by DNA glycosylases, such as the activation-induced deaminase (AID) or the apolipoprotein B mRNA editing enzyme catalytic polypeptide 1 (APOBEC1) (Jacobs & Schär, 2012).

Just like passive demethylation, active demethylation also plays a significant role in the processes after fertilization (Eckersley-Maslin et al., 2018; Guo et al., 2014; Seisenberger et al., 2013). As mentioned above, especially the paternal genome undergoes a post-fertilization demethylation. However, in other contexts, not only genome-wide demethylation, but also locus-specific active DNA demethylation has been previously described. For example, the locus-specific demethylation occurring in the adult brain (D. K. Ma et al., 2009).

2.2.3 Methylation in sperm and oocytes

The DNA methylation level is not the same in all cells or tissues. This is also true for the gametes, female oocytes and male sperm. During mammalian development, primordial germ cells (PGCs) undergo a global wave of DNA demethylation at the time of reaching the gonadal ridge (Saga, 2008). Precursor cells start to migrate from the proximal epiblast. From this moment on, the level of DNA methylation gradually decreases in both male and female PGCs (Guibert et al., 2012). In females, some germline-specific genes and X-linked genes are

demethylated (Hackett et al., 2013). The methylation loss continues until it reaches 3 – 4% of original level (Kobayashi et al., 2013). After gonadal sex determination, DNA methylation patterns have to be established in each germ cell in a sex-specific manner (Sakai et al., 2004).

As mentioned above, CGI is a region with high concentration of CpG dinucleotides. There are exclusively oocyte-specific and sperm-specific methylated CGI. However, several CGI are methylated in both oocytes and sperm (Kobayashi et al., 2012). In the oocyte, a close relationship between gene-body DNA methylation and gene expression was described by Kobayashi et al. In the sperm, the correlation of gene-body methylation and gene expression was not as obvious as in oocytes. This is probably caused by the genome-wide hypermethylation which is typical for the male gametes (Kobayashi et al., 2012). In sperm both CpG and non-CpG methylation can be observed (Ichiyanagi et al., 2013). In fully mature murine spermatozoa, the global CpG methylation level excluding the CGIs reaches almost 90% (Donkin & Barrès, 2018).

The epigenome in sperm cells is very different to the one of somatic cells (Chong et al., 2007). This is characterised especially by genome-wide DNA methylation pattern, which is typical for the sperm (Godmann et al., 2009). The correct methylation establishment is important for proper sperm function as, among others, proper DNA methylation correlates with sperm chromatin condensation (Marques et al., 2010). One example of methylation function in sperm would be imprinting. Inappropriate imprinting might lead to infertility (Hajj et al., 2011).

In contrast to the sperm, mature oocytes show genome-wide CpG methylation in only 40% in non-CGI regions (Kobayashi et al., 2012). The DNA is methylated gradually throughout development and growth of the oocyte. The major phase of *de novo* methylation occurs in growing oocytes (Smallwood et al., 2011). Beside DNMT3a and DNMT3b, which secure *de novo* methylation, there is also DNMT3L in oocytes, which participates in DNA methylation. DNMT3b does not seem to be important for oocytes (Smallwood et al., 2011). Also in oocytes, one of the important roles of methylation is imprinting. Defects in imprinting caused by loss of DNA methylation leads to mouse embryonic lethality (Tucci et al., 2019). Methylation is dispensable for oocyte development or fertilization, but the imprinting is essential for embryonic development. Complete loss of DNA methylation in oocytes leads to embryonic death (Kaneda et al., 2004).

2.3 DNA methylation after fertilization

The fertilization is a process when the female oocyte and male sperm fuse together and create one cell: the zygote. After fertilization, in conjunction with the establishment of totipotency, many epigenetic changes occur. However, unlike the maternal genome, which is associated with histones throughout oogenesis and the final steps of oocyte maturation, the sperm genome must be substantially transformed.

Approximately one hour after fertilization, the paternal genome undergoes major chromatin remodelling. During this process, protamines are lost and they are replaced by maternal histones and the paternal pronucleus is formed (McLay & Clarke, 2003). In mammals, the zygote contains two separate haploid parental pronuclei. In mice, the maternal and paternal pronuclei can be distinguished based on the size of the pronuclei, where the paternal one is the larger one. The period of development after fertilization can be described by the pronuclear stages (PN): PN1 – PN5 (Adenot et al., 1997).

In accordance with protamine-histone transition, DNA demethylation also takes place after fertilization. The dynamics of demethylation in pronuclei after fertilization is not the same between the maternal and paternal one. Passive demethylation happens gradually and occurs predominantly in the maternal pronucleus (Rougier et al., 1998). DNA methylation inherited from the oocytes is erased during cleavage division, most likely because of exclusion of DNMT1 from the nuclei (Messerschmidt et al., 2014).

On the other hand, active demethylation is the dominant process of genome-wide DNA demethylation of the paternal pronucleus in the zygote. The rapid loss of paternal methylation takes place in a couple hours before the first DNA replication, and this is the reason why it is called replication-independent demethylation. Replication in the paternal pronucleus starts after rapid loss of DNA methylation. As mentioned, the oxidation of 5mC by TET enzymes was confirmed to be involved in the active demethylation of the paternal genome (Gu et al., 2011; Iqbal et al., 2011). TET enzymes will be described in more detail in the next chapter. The conversion of 5mC in the paternal pronucleus starts at 4–6 hours after fertilization. Main decrease of 5mC level occurs at PN3 (Santos et al., 2013).

The maternal genome is protected from the active demethylation by binding of a protein called Developmental pluripotency-associated protein 3 (DPPA3), also known as

PGC7/STELLA. This protection is important for imprinted genes and epigenetic asymmetry (Nakamura et al., 2007).

The global demethylation continues through the preimplantation development until the blastocyst stage. Then the methylation pattern is re-established depending on the nascent tissue type. This wave of DNA demethylation is conserved in mice and humans, but it does not occur exclusively in these species (Iurlaro et al., 2017). DNA demethylation of the paternal genome after fertilization is mainly facilitated by the maternal factors. DNA demethylation and other processes happening after fertilization are summarised in Figure 1.

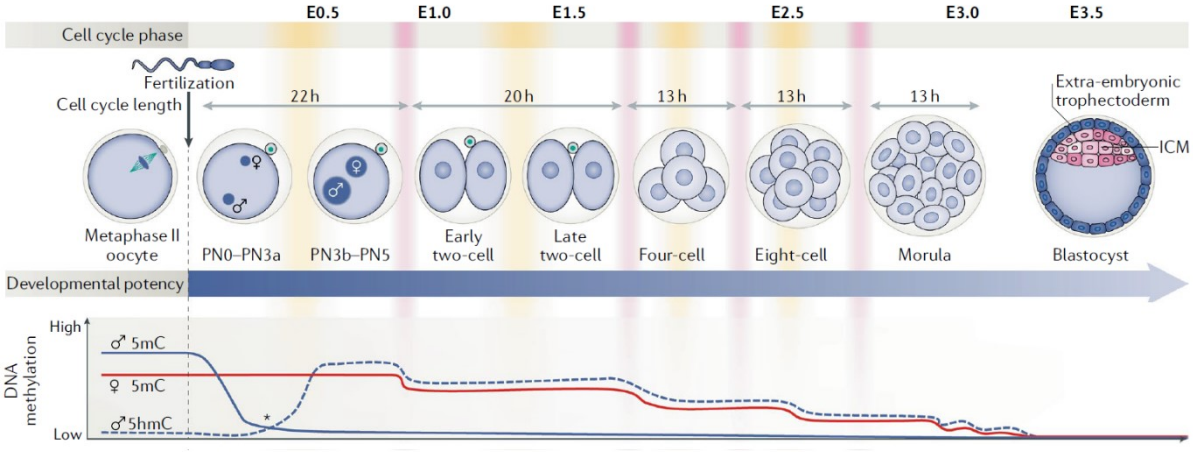

Figure 1 Overview of remodelling and reprogramming dynamics after fertilization. TOP: Yellow bars represent DNA replication, S phase, while red bars represent M phase**.** After fertilization, two pronuclei are formed and based on their structure, PN stages can be defined. Using PN stage characteristics of zygote can be described. At PN0 – PN3 protamines are replaced by maternal histones and the main wave of demethylation occurs. BOT: Dynamics of DNA methylation. Blue represents paternal DNA methylation, red maternal DNA methylation. Maternal DNA methylation is lost gradually through the replication. Paternal DNA methylation is lost shortly after fertilization and before first DNA replication. Approximate embryonic days (E) are denoted. Modified from Eckersley-Maslin et al., 2018.

2.3.1 Maternal factors involved in paternal DNA demethylation

Several important maternal factors involved in paternal DNA demethylation have been found. However, the full list of all the maternal factors is still not complete. Some of the most important maternal factors are described in the following chapters.

2.3.1.1 Ten-eleven translocation (TET) enzymes

TET enzymes were proposed to oxidize 5mC and 5m pyrimidine and Iyer et al. predicted that TET enzymes act preferentially on the 5mC (Iyer et al., 2009). Such prediction

was confirmed, and it was shown that TETs enzymes oxidized 5mC to 5hmC (Tahiliani et al., 2009). Furthermore, it has been presented that TETs do not only oxidize 5mC to 5hmC, but the oxidation reactions continue to carry out 5fC and 5caC (Ito et al., 2011).

The TET family of proteins has three members in mammals: TET1, TET2, TET3 (Iyer et al., 2009). TET1 is highly expressed at the stage of morula. mRNA for TET2 appears from the zygotic genome activation through the stage of blastocyst. mRNA for TET3 can be detected mainly at the zygotic stage and then it starts to disappear (J. Y. Ma et al., 2014).

Each of the TET enzymes has a carboxyl-terminal catalytic core region comprising a Cys-rich domain and a double-stranded β helix (DSBH) fold and belong to the 2OGFe-dioxygenase (2-oxoglutarate (also known as α-ketoglutarate) and Fe (II)-dependent dioxygenase) superfamily. All members of this superfamily utilize 2OG, reduce iron and both atoms of molecular oxygen, to generate their oxidised substrates (Iyer et al., 2016). In the case of the TET family, oxidised products are 5hmC, 5fC and 5caC.

As previously mentioned, the main role of mammalian TET proteins is to enable DNA demethylation through the oxidation of 5mC. It was suggested that TET mediated 5mC oxidation participates in the active demethylation process after fertilization (Gu et al., 2011; Iqbal et al., 2011; Wossidlo et al., 2010). All oxidized forms of 5mC can be also lost through passive dilution, replication-dependent mechanisms. The summary is depicted in Figure 2.

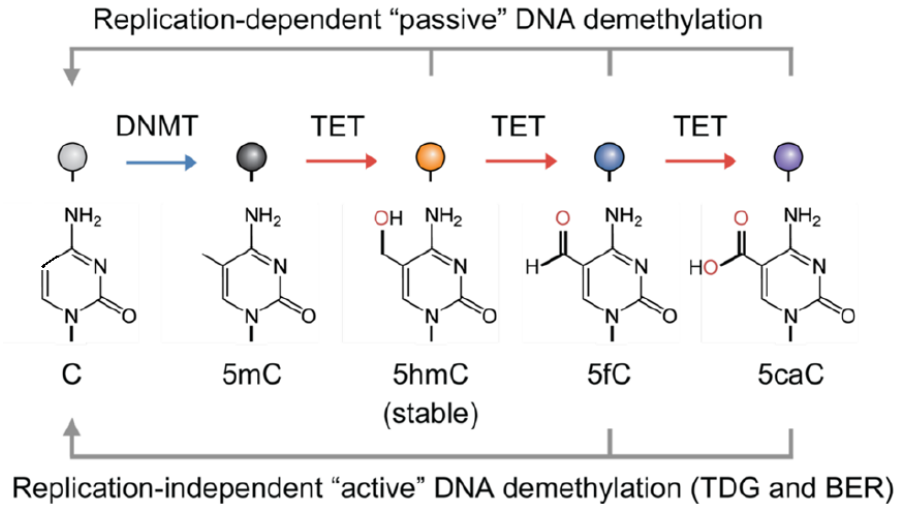

Figure 2 Following modifications of 5mC after oxidation by TET enzymes. TET is able to oxidize 5mC to 5hmC and this changes its chemical characteristics. Oxidation continues with 5fC and 5caC. Oxidized forms of 5mC can be detected as DNA damage by the cell and removed by a repair mechanism. Alternatively, these forms can also remain in DNA and they might be lost gradually through dilution. Adapted from Lio et al., 2020

As previously stated, TET3 can mainly be found in zygotes, which makes it the main player of the TET family in the active demethylation (Wossidlo et al., 2010). At the zygotic stage, TET3 is concentrated in the male pronucleus but it translocates to the cytoplasm in the later preimplantation stages (Gu et al., 2011). The levels of 5hmC increase with the TET3 enrichment in zygotes (Gu et al., 2011; Iqbal et al., 2011; Wossidlo et al., 2010). Zygotes deficient in TET3 show disrupted conversion of 5mC to 5hmC in the paternal genome and deceleration of demethylation of several paternal genes, (Gu et al., 2011). Moreover, the reduction of TET enzymes leads to hypermethylation in embryonic development (Dawlaty et al., 2014).

It was detected that the generation of 5fC occurs from PN3 until PN5 (C. Zhu et al., 2017). This is in compliance with the situation that the conversion of 5mC starts 4–6 hours after fertilization (Santos et al., 2013). This leads to the suggestion that the active demethylation by TET3 enzymes occurs at later zygotic stages and not right after fertilization.

As mentioned, it is believed that the maternal pronucleus is protected from active demethylation by PGC7/STELLA (Nakamura et al., 2007). However, the presence of s 5hmC and 5fC was detected in the female pronucleus as well, suggesting that TET3s might also act in the maternal pronucleus (Shen et al., 2014).

After TETs acting, oxidized bases are created at the place of the original 5mC. This can lead to inappropriate pairing and can be recognised as a mistake. Cells have to fix these mismatches and for that repair mechanisms are needed.

2.3.1.2 Thymine DNA glycosylase

Thymine DNA glycosylase (TDG) is an enzyme, which is able to recognise GT mismatches and induce the repair mechanisms (Neddermann et al., 1996). TDG also has the ability to remove 5fC and 5caC from DNA strands (Maiti & Drohat, 2011). The loss of TDG leads to an accumulation of 5fC and 5caC (Shen et al., 2013). TDG activity could be an additional step following the TET3 active demethylation, because 5hmC and the oxidised derivatives do not spontaneously convert to unmodified cytosine (Lio et al., 2020). They can be lost through replication or repair. The process after TDG acting might further continue with BER. In accordance with this repair mechanism, 5fC and 5caC are replaced by unmodified C (He et al., 2011; Maiti & Drohat, 2011). BER is described later in more detail in the following chapter.

2.3.2 Base excision repair

After the active loss of 5mC via processing by TET3, the genome contains with oxidized forms of 5hmC, 5fC and 5caC. As it was already mentioned, these forms can be more easily recognized and excised from DNA by enzyme TDG. Removing these bases leaves a lesion in DNA, abasic sites (AP, apurinic/apyrimidinic site), which have to be repaired (Maiti & Drohat, 2011). This suggests that another step in active demethylation is BER. Indeed, it was proposed that active demethylation after fertilization in mice involves BER (Santos et al., 2013; Wossidlo et al., 2010).

BER is a cellular multienzyme system for correcting small base lesions which are usually non-helix-distorting (T. H. Lee & Kang, 2019). In general, this repair mechanism participates in the maintenance of the genome integrity, which is challenged by exogenous factors or by the cell's own metabolism on a daily basis (de Bont & van Larebeke, 2004).

BER can be divided into two subpathways: short-patch, where a single nucleotide is removed, and long-patch, where two and more nucleotides are repaired (Fortini & Dogliotti, 2007; Robertson et al., 2009). Both pathways can be defined by three major steps: First, lesion recognition, second, excision of the damaged nucleotide and third, re-synthesis using error-free DNA polymerases (T. H. Lee & Kang, 2019). BER is initiated by DNA glycosylases, such as the afore mentioned TDG, which creates DNA lesions in accordance with the mismatches in DNA, which needs to be repaired (Jacobs & Schär, 2012). This is followed by the action of another major core protein, AP-endonuclease, which can detect the AP-site. AP-endonuclease is responsible for DNA strand incision and creating a gap in double-stranded DNA (Esadze et al., 2017). After AP-endonuclease acting, in the DNA strand rest the single-nucleotide gap. This can be detected by one of many DNA polymerases, which are able to use the single strand as a template and fill the gap. The main DNA polymerase which participates in BER is DNA Pol β. The last BER participant is the DNA ligase. Specifically, to the BER activity DNA ligase I and III are linked (T. H. Lee & Kang, 2019).

Next to TDG, there are other DNA glycosylases participating in BER such as the Methyl-CpG-binding domain protein 4 (MBD4). MBD4 was originally suggested to be the demethylase in zebrafish (Rai et al., 2008). TDG and MBD4 can remove both U and T unfitting with G (Hendrich et al., 1999).

Beside DNA glycosylases there is another group of enzymes which can induce BER. Enzyme activation-induced deaminase (AID) as well as TETs changes the chemicals of 5mC and catalyses the deamination of 5mC to create T (Bhutani et al., 2010; Rai et al., 2008). AID was described as a demethylation partner for MBD4. It was proposed that deamination by AID, followed by thymine base excision repair by MBD4 led to the DNA demethylation (Rai et al., 2008). AID can also deaminate C to create U. Created mismatches are recognized by one of mentioned DNA glycosylase and the unfitting base is removed. (Morgan et al., 2004). Participation of described factors connected to BER are depicted in Figure 3.

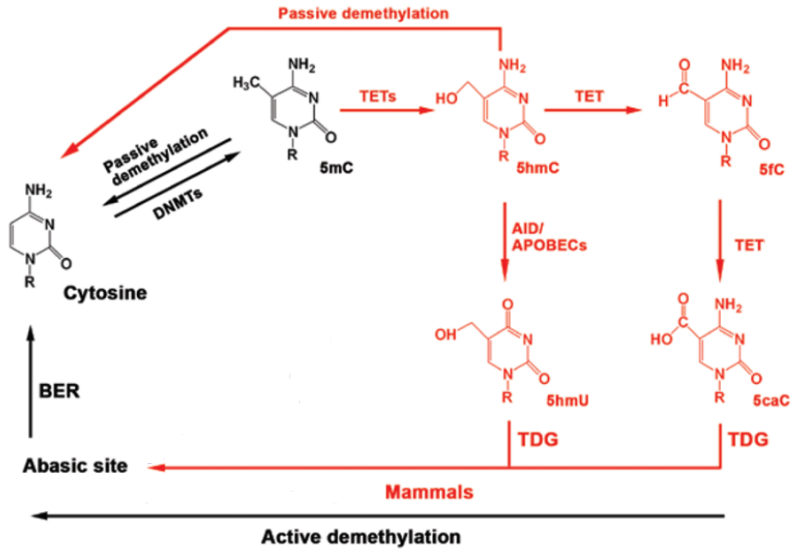

Figure 3 Overview of the connection between TET oxidation, TDG and BER activity. 5mC is created from C by DNMTs in "one step". But the reverse process is longer and includes modification of 5mC, recognition of this modification and removal of the unfitting base creating a lesion in the DNA strand. This nick is fixed by repair mechanisms. Modified from Gong & Zhu, 2011.

It was presented that several steps of active demethylation in murine zygotes possibly involve AID-mediated cytosine deamination coupled with BER long-patch intermediate (Santos et al., 2013). Moreover, in the context of long-patch BER, 5mC can be replaced directly by an unmethylated cytosine in the process of repair of the neighbouring lesions; the 5mC does not have to be specifically recognized. Unfortunately, the molecular mechanism of the process of AID-mediated long-patch repair in this process remains unknown.

Interestingly, in mammalian cell lines it has been proposed that not only AID, but also DNMT3a and DNMT3b are able to deaminate the 5mC and generate T. As mentioned, T

mismatch might be recognized by TDG and removed by repair enzymes machinery. Moreover, it was described that TDG associates with DNMT3a and DNMT3b (Boland & Christman, 2008).

It was proposed that at the time of paternal DNA demethylation in mice, DNA double- and single-stranded breaks are generated. DNA breaks were detected by histone variant γH2A.X, which localizes into dsDNA breaks (Wossidlo et al., 2010). In accordance with the BER involvement, inhibition of the BER components PARP1 and AP-endonuclease affect paternal DNA demethylation (Hajkova et al., 2010). Altogether, these observations suggest that DNA breaks are in fact created during zygotic reprogramming.

As mentioned in chapters above, protein PGC7/STELLA can bind to the maternal genome and protect it from active demethylation (Nakamura et al., 2007). Analysing the BER activity in the PGC7/STELLA null zygotes it was observed that the activity of BER components is detectable in both maternal and paternal pronuclei, which were first accumulated in paternal pronucleus (Hajkova et al., 2010). This points to the possibility that activation of BER is connected to DNA demethylation and that the repair mechanism may end up with replacement of 5mC and its derivatives with unmodified cytosine (Hajkova et al., 2010; Santos et al., 2013).

Chapters above describe processes and factors connected to DNA demethylation and its connection to the repair mechanisms. All of these are maternally derived factors and they accumulate in oocytes prior to fertilization.

2.4 Oocyte germinal vesicle

During the development of oocytes, oogenesis, oocytes are arrested at the diplotene stage of prophase I from birth prior to ovulation, when the oogenesis continues. At this period the oocytes are called a primary oocyte. Nucleus of the immature oocyte is called a germinal vesicle - GV (Gilbert, 2014).

As in somatic cells, the GV is lined by a nuclear membrane (NM), which is supported by the layer of nuclear lamina (NL) composed of lamin proteins positioned between the chromatin and inner nuclear membrane. Inside of the nucleus, there is a nucleoplasm consisting of a wide range of proteins. In Xenopus, the GV proteins were classified into two categories based on the solubility differences (Merriam & Hill, 1976). The first category is composed of soluble or easily solubilized proteins. These proteins comprise 87% of the

nucleoplasm and are similar to soluble proteins of the cytoplasm, but still unique for the nucleus. The residual proteins of the nucleoplasm are tightly bound to a nucleoplasmic gel, which is the structure in the nucleoplasm, or nuclear organelles (Merriam & Hill, 1976).

About 97% of GV proteins are associated with the nuclear gel while 3% of the total mass of GV proteins contribute to the nuclear structure formation (Merriam & Hill, 1976). The GV structural proteins are classified as the insoluble fraction. Both fractions are very important for the period after fertilization and embryonic development.

During meiotic maturation of oocyte, GV undergoes the GVBD and the GV components are released to the cytoplasm. After GVBD, chromosomes condense and create the meiotic spindle in the assistance of cytoskeleton. During metaphase of meiosis I (MI), half of the chromosomes are excluded, and the first polar body is formed. At this moment of metaphase arrest II (MII), the oocyte is ready to be fertilized (Gilbert, 2014).

2.4.1 Lamins, component of GV insoluble fraction

Very important proteins of the nuclear envelope are lamins, cytoskeletal proteins belonging to a group of intermediate filaments. They represent a separate type V intermediate filament. These proteins can form a dense protein network, NL, which adjoins the inner NM (Dittmer & Misteli, 2011). Lamins interact with both NM and chromatin inside the nucleus, thus it has been proposed that lamins participate in DNA replication, transcription, cell proliferation and differentiation (Dechat et al., 2008).

There are two main types of lamins, type A and type B. Type A lamins include two proteins, lamin A and lamin C. Both are encoded by the same *Lmna* gene, which is differentially spliced to produce two separate proteins (Stewart & Burke, 1987). Type A lamins are abundantly expressed in differentiated cells (Rober et al., 1989). They serve as a structural support for the nuclear envelope and are thought to be the main proteins determining the stiffness and elasticity of the nuclear membrane (Yabuki et al., 1999). The type B lamins include two proteins, lamin B1 and lamin B2, each encoded by its own gene, *Lmnb1* and *Lmnb2*, respectively. Unlike type A, type B lamins are ubiquitously expressed (Davies et al., 2011). Lamin B is not as involved in the nuclear envelope stiffness as lamin A/C, however, they are important for anchoring the nucleus to the cytoskeleton, and nucleus migration (Lammerding et al., 2006).

Mutations in the *Lmna* gene lead to many diseases called laminopathies (Rankin & Ellard, 2006). In contrast to the *Lmna* genes, fewer diseases connected to the *LMNB* gene have been described. *Lmnb* gene mutations can be lethal at birth or even at prenatal stage (Vergnes et al., 2004).

Genome regions which are in contact with the NL are called lamina-associated domains (LADs). They have been identified in different species including mouse and human. Genes of these regions are mostly transcriptionally silenced, or the expression occurs at a very low level. In general, LADs are related to heterochromatin (Guelen et al., 2008; Peric-Hupkes et al., 2010). LADs have been identified in both GVs and zygotes. After fertilization, LADs are established *de novo*. Maternal and paternal LADs are established asymmetrically (Borsos et al., 2019). This might correlate with different epigenetic changes in parental pronuclei after fertilization.

As all lamins, lamin A/C and lamin B, are present in unfertilized GV oocyte, lamin A/C seems to be gradually depleted prior to the 8-cell stage and blastocysts stage (Houliston et al., 1988). On the other hand, it is likely that lamins inherited from oocytes play their role in the parental pronuclei formation (Ogushi et al., 2005). However, lamins are not only structural proteins, but they might also play a role in the DNA damage repair.

2.4.1.1 The role of lamin A/C in DNA repair

As it was already mentioned, mutations in the LMNA gene lead to diseases commonly named laminopathies. Symptoms connected to these diseases are associated with defects in DNA repair (Worman, 2012; Worman et al., 2010). There are two major pathways of double strand break (DSB) repair occurring in mammalian cells, homologous recombination (HR) and non-homologous end-joining (NHEJ). A-type lamins participate in both repair pathways (Redwood et al., 2011).

Nevertheless, it was proposed that lamin A/C can also participate in DNA single-strand breaks repair. Maynard et al. have suggested that lamin A/C has a role in the BER pathway as well (Maynard et al., 2019). The authors showed that lamin A/C knockout mouse embryonic fibroblasts (MEF) cells and lamin A/C knockdown U2OS cells, human bone osteosarcoma epithelial cells, exhibited an accumulation of 8-oxoguanine, which is one of the most common DNA lesions resulting from reactive oxygen species (ROS) (Kanvah et al., 2010) and an

increased frequency of substitution mutations (Maynard et al., 2019). Under normal circumstances, 8-oxoG is repaired by the BER pathway (Whitaker et al., 2017). However, the details of how lamins participate in the repair process remain unknown. The model of MEF cells (mouse), and U2OS (human), cell lines typically used in research in stem cell biology or biomedicine (Niforou et al., 2008; J. Xu, 2005), underscore the importance of lamin A/C in BER-based DNA repair and indicate that this role might be conserved among mammals. In my thesis, I wanted to investigate, whether lamin A/C participates in BER in general, or is specific to the 8-oxoG repair, and whether its positive influence on BER is direct or indirect, e.g. by influencing the level of gene expression of the BER components. To achieve these goals, I have used the model of early mouse embryos, which are highly equipped for BER, yet the changes in gene expression are minimal.

3 Aims of thesis

- Verifying the methylation level of chosen DNA sequences.
- Compare the difference of the methylation level between the situation before and after fertilization.
- Determinate the amount of protein lamin A/C per one GV oocyte using a suitable method.
- Using the method selective enucleation, observe the situation after fertilization without the insoluble fraction. To the system add protein lamin A/C and compare.

4 Material

4.1 Biological material

Swiss female mice, NMRI male mice, 3 – 10 weeks old, ordered from Janvier LABS in France.

4.2 Laboratory devices

Name	*Supplier*
ARE Heating magnetic stirrer	Velp scientifica
Autoclave	Biobase, class B
Azure 300 Imager	Azure biosystems

Carl zeiss Jena microscope	Leitz, WIld heerbugg, hergestellt in der DDR
Centrifuge	Eppendorf, 5430 R
Cycler	Applied Biosystems™ ProFlex™ PCR System
Electrophoresis power supply	Consort, E844
Freezer	Binder, 9020-0347
Fume cupboard	Q pol lab Q dynamic, AORE 1500
Germinator 500	CellPoint Scientific Inc. 2191
Heating plate	Vezas, Czech Republic
Incubator	Sanyo O_2/CO_2
Laboratory scales	Precisa Instruments, XT 220A
Microwave	Daewoo
Mixer	IKA, KS 130 control
Mixing Block	BIOER, MB-102, SN BYQ6008E-250
Nanodrop™ 2000	ThermoFisher Scientific, ND2000CLAPTOP
Oven mino	Genlab, 6L CLAD. INT. 250ºC, OV160-05
Pipette	Nichipet Premium
Plus II Incubator	Gallenkamp, IPLO75WT1C
power supply	Consort, Electrophoresis power supply
TE 22 Mighty Small Transfer Tank	Hoefer, TE22
UVP transilluminator	Analytik jena, UVP PhotoDoc- It imaging system
Vortex Mixer	P-lab

4.3 Laboratory consumables

Name	*Supplier*
4-Well Dishes	ThermoFisher scientific, 179830
50 ml conical tube	Falcon 352098
Centrifuge tube	TPP, 91015
epTIPs Standard µl	Eppendorf, 0030000.919
epTIPs Standard 2-200 µl	Eppendorf, 0030 000.870
Glass capillary	Hirschmann, 9600150
Hypodermic needles	Medoject
Micro tips 10 µl	Neptune, 2040
Microtitration plate	Gama, V400919
Mini-PROTEAN ® comb 15-well	Bio-Rad, 1653360
Mini-PROTEAN ® Glass plates	Bio-Rad, 1653311
Mini-PROTEAN ® Short plates	Bio-Rad, 1653308
Needles	KDM, 900260
Petri dishes 10 mm	Falcon, 351008
Petri dishes 60 mm	Gama, V400927
Phase Lock Gel Heavy 2.0 ml	Eppendorf, 955154045
pH Test Strips 0.0-6.0	Sigma chemical company, P-4661
PVDF membrane	Cytiva Amersham™
Screw cap tubes	Delta lab
Tube 15 cm	Gama, V 400941

4.4 Commercial kits

Name	*Supplier*
QIAprep ® Spin Miniprep Kit (250)	QIAGEN, 27106
RNeasy ® Mini Kit (250)	QIAGEN, 74106
TGX FastCast Acrylamide Kit, 10%	Bio-Rad, 1610173

4.5 Chemicals

Name	*Supplier*	*Catalogue Number*
10X PCR buffer	HighQu	
Agarose SERVA Wide Range	SERVA	CAS 9012-36-6
Ammonium persulfate analytical grade	Serva	13375.01
B-mercaptoethanol	Sigma	200-464-6
Blotting Grade Non-Fat Dry	Bio-Rad	170-6404
Calcium chloride dihydrate	Sigma	C7902
Disodium hydrogen phosphate	Penta	15140-31000
dNTPs MIX 20mM each	Solis BioDyne	02-31-00020
ECL Advance ™ blocking agent	Amersham ™ GE Healthcare UK Limited	CPK1075
ECL Select ™ Wester Blotting Detection REAGENT	Amersham ™ GE Healthcare UK Limited	RPN 2235
Ethanol 96%	Penta	Cas 64-17-5
EDTA	Sigma-Aldrich	03690
FastRUler ™ DNA Ladder	Fermentasion	SM1103
Glucose	Sigma	G6152
Glutathione	Sigma	G4251
Glycine	Bio-Rad	161-0724
Glycogen	Invitrogen	10814010
HEPES	Sigma	7365-45-9
hCG, Sergon 500 IU/ml	Bioveta	
Hydrochloric acid 35%	Penta	CAS 7647-01-0
Hydroquinone	Sigma-Aldrich	H17902-100G
IBMX	Sigma-Aldrich	I5879-250MG
Isopropanol	Penta	CAS 67-63-0
EmbryoMax® Advanced KSOM Embryo Medium	Sigma-Aldrich	MR-101-D
Laemmli sample Buffer	Bio-Rad	161-0737

Lamin A/C (H-110), rabbit polyclonam	Santa Cruiz	Sc-20681
M2 with hyaluronidase	EmbryoMax ®	MR-051-F
Magnesium sulfate heptahydrate	Sigma	M7774
Methanol	Merck	1.06009.2511
Methyl-β-cyclodextrin	Sigma	C4555
MgCl	HighQu	
Midori Green Advance DNA Stain	Genetics	MG04
Minimum Essential Medium	Sigma	M4655
N,N,N´,N´-Tetramethyl-ethylenediamine	Serva	CAS 110-18-9
Na-lactate	Sigma	L7900
Na-pyruvate	Sigma	P4562
Penicillin G	Sigma	P4687
PMSG, Folligon	MSD Animal health	
Polyvinylalcohol	Sigma	P8136
Potassium chloride	Sigma	P5405
Potassium phosphate	Sigma	P5655
Proteinase K Solution	5 Prime	Mat 2900146
Proteinase inhibitor MIX	SERVA	39102.01
RIPA buffer	TermoFisher	FNN0021
Siliconol M 1OO	Roth	Art.-Nr- 4025.1
Sodium acetate	Sigma-Aldrich	S5636-250G
Sodium bicarbonate	Sigma	S5761
Sodium chloride	Emprove	K42468700
Sodium chloride	Sigma	S5886
Sodium dodecyl sulfate	Sigma-Aldrich	L3771-1KG
Sodium hydroxide pellets	Penta	CAS 1310-73-2
Sodium metabisulfite	Sigma-Aldrich	31448-500G
Streptomycin	Sigma	S1277
Taq DNA polymerase	HighQu	PCE0202
TBE Buffer	Merck	1.06177.2500
Tris Base, Molecular Biology Grade	Calbiochem	648310
TWEEN ®	MP Biomedicals, LLC	194841
Vaseline weiss	Roth	Art.-Nr. 5775.1
Water	Sigma	W4502, CAS 7732-18-5

4.5.1 Solutions

4.5.1.1 Buffers

3M NaOH		
Chemicals		
NaOH		0,2 g
dH_2O		1,66 ml
3M NaOAc		
Chemicals		
NaOAc		2,46 g
dH_2O		8 ml
HCl		-> pH 5,2
dH_2O		up to 10 ml
Lysis buffer		
Chemical	*Final concentration*	*Volume ml*
1M Tris pH 8	10 mM	0,05
5M Nacl	100 mM	0,1
0,5M EDTA pH 8	10 mM	0,1
10% SDS	0,5%	0,25
dH_2O		4,5
PBS 10X		
Chemicals		*g / 1l*
NaCl		80
KCl		2
Na_2HPO_4		14,4
KH_2PO_4		2,4
dH_2O		800 ml
HCl		-> pH 7,4
dH_2O		up to 1l
Reconstitute buffer		
Chemical	*Final concentration*	*g*
Tris	20 mM	2,42
NaCl	150 mM	8,76
dH_2O		up to 900 ml
5 M NaOH		-> pH 8
dH_2O		up to 1l
TE buffer		
Chemical	*Final concentration*	*Volume ml*
1 M Tris-HCl	10 mM	0,1
0,5 M EDTA pH 8	0,1 mM	0,002
dH_2O		up to 10 ml

4.5.1.2 Media

HTF	
Chemical	*mg / 100ml*
NaCl	593
KCl	35
D (+) Glucose	55
KH_2PO_4	5
$MgSO_4$ x 7 H_2O	5,1
CaCl2 x 2 H_2O	30
D-L- Na Lactate	236,34
Gentamicin Sulfate	1
Na-Pyruvate	3,7
$NaHCO_3$	33
HEPES	477
dH_2O	up to 100 ml
TYH	
Chemical	*mg / 100ml*
NaCl	697,6
KCl	35,6
$MgSO_4$ x 7 H_2O	29,3
KH_2PO_4	16,2
$CaCl_2$ x 2 H_2O	25,1
Na-Pyruvate	5,5
Glucose	100
Methyl-β-cyclodextrin	98,3
Penicillin G	7,5
Streptomycin	5
$NaHCO_3$	210,6
PVA	100
dH_2O	up to 100 ml

4.5.1.3 Western Blot buffers

Running buffer – Tris-Glycine-SDS 0,1% 10X	
Chemical	*g / 1l*
Tris Base	30,2
Glycine	144,2
SDS	1
dH_2O	up to 1l
Transfer buffer (Towbin) – Tris-Glycine 10X	
Chemical	*g / 1l*
Tris Base	30,275

Glycine	144
dH_2O	up to 1l
Tris Buffered Saline – TBS 10X	
Chemical	*g / 1l*
Tris Base	24
NaCl	88
dH_2O	900 ml
HCl	-> pH 7,6
dH_2O	up to 1l
Running buffer – Tris-Glycine-SDS 0,1% 1X	
10X stock	100 ml
dH_2O	900 ml
Transfer buffer (Towbin) – Tris-Glycine 1X	
10X stock	100 ml
MetOH	100 ml
dH_2O	800 ml
Tris Buffered Saline – TBS 1X / TBST 0.05%	
10X stock	100ml
Tween	500 µl
dH_2O	up to 1l

4.5.2 Proteins

Name	*Supplier*	*Catalogue Number*
recombinant protein Lamin A/C	Cloud-Clone Corp	RPF550Mu01
Primary antibody against lamin A/C	Santa Cruiz	Sc-20681
goat anti-rabbit antibody	Abcam	ab6721

5 Methods

5.1 Mouse manipulation

For collecting the material for samples, 3 – 10 weeks old Swiss female mice and NMRI male mice were used. Mice were ordered from Janvier LABS in France.

Hormone stimulation was administered in a form of injections into the peritoneum of female mice to ensure abundance of GV, MII, and zygotes. All mice were sacrificed by cervical dislocation.

5.1.1 Sperm sample collection

For sperm collection, male cauda epididymis was removed. The sperm dish was prepared: 200 µl of TYH medium (see chpt. Material) was dropped into a dish and covered with mineral oil (Roth). Cauda was transferred into the oil, cut open which allowed for the sperm to be released and introduced into the drop of TYH medium. The dish was placed in an incubator for 20 - 30 minutes to let the sperm spread around the whole drop. From 75 µl to 100 µl of sperm drop was taken, washed in 1X PBS (see chpt. Material) and spun down. The pellet was stored at – 20°C or used directly for further experiments.

5.1.2 Oocyte sample collection

5.1.2.1 GV oocyte

For collecting GV, 7 IU of PMSG (MSD Animal health) was injected typically around 12 PM. The isolation was done 46 – 48 hours after injection.

The female ovaries were removed and put into a drop of HTF medium (see chpt. Material) containing an inhibitor IBMX (isobutyl-methylxanthine, Sigma-Aldrich). The ovaries were minced using thick needles and GVs themselves were collected by fine glass capillary. For bisulfite sequencing, 10 to 20 GVs were collected in 1 µl of HTF medium. For WB, GVs were washed in PBS with 0,1% PVA (polyvinylalcohol, Sigma) first and from 20 up to 60 GVs were collected in 2,5 µl of PVA. For BS, samples were stored at –20°C. For WB, samples were stored at -80°C.

5.1.2.2 MII oocyte

For MII collection, the super-ovulated female mice were needed. 7 IU of PMSG was injected typically between 5 – 6 PM. After 48 hours, 7 IU of hCG (Bioveta) was injected. The isolation was done 14 – 16 hours after the last injection.

The female oviducts were removed and put into a drop of HTF medium. Using forceps and syringe needle the ampulla was opened and the cumulus-oocyte-complexes (COCs) were released into the drop of medium. Another dish was prepared with 50 µl drop of M2 medium with hyaluronidase (EmbryoMax ®) and four 200 µl drops of fresh HTF medium. With 100 µl pipette the COCs were removed into the M2 medium with hyaluronidase and kept on the warm plate for 1 minute for releasing the MII oocytes from cumulus cells. After that, oocytes were washed four times in HTF medium drops. From 10 up to 20 MII oocytes were collected in 1 µl of HTF medium and stored at – 20°C.

5.1.3 Zygote collection

For zygotes collecting, 7 IU of PMSG was injected typically at 12 PM. After 48 hours, 7 IU of hCG was injected and females were introduced to the male for mating one female per one male. After 20 hours the females were checked for vaginal plugs. If positive, the collection of zygotes was performed after another 5 hours.

The female oviducts were removed and put into a drop of HTF medium. The zygotes were found in one of the following situations. First, one-cell zygotes were in a compact complex in ampulla. Second, single one-cell zygotes were dispersed along ampulla. In the first scenario, the same way of harvesting as for MII oocytes was used (hyaluronidase dish). For the second scenario, the zygotes were pushed out of the ampulla using two syringe needles. Single zygotes were picked by fine glass capillary and washed three times in fresh THF medium. From 10 up to 20 zygotes were collected in 1 µl of HTF medium and stored at – 20°C.

5.2 Isolation of DNA from gametes and zygote samples

5.2.1 DNA isolation from sperm sample

The isolation of sperm DNA was based on the work of Wu and his group (H. Wu et al., 2015). For samples, 100 µl of TYH medium containing sperm was collected. Aliquots were centrifuged and supernatant was removed, the pellets were washed in 1X PBS, followed either by the DNA isolation itself or their storage in -20°C until further use. On the day of the experiment, pellets were resuspended in 15 µl of β-mercaptoethanol (Sigma), 15 µl of proteinase K (20 mg/ml, 5 Prime) and 720 µl of lysis buffer (see chpt. Materials). The samples

were incubated at 55°C for 3 hours in a mixing block. After that, isolated DNA was purified using phenol-chloroform extraction. The sample was transferred to the Eppendorf tube Phase lock gel heavy (Eppendorf) and phenol was added in a 1:1 (sample:phenol) ratio. Samples were centrifuged for 10 minutes at 12 000 g. This process was repeated twice. Then the supernatant was transferred to a clean 2 ml Eppendorf tube and the same volume as supernatant of chloroform was added, followed by centrifugation at 12 000 g for 10 minutes. The bottom phase was then removed, fresh chloroform added, and samples were centrifuged once again, and the upper phase was transferred to a new tube. Purified DNA was precipitated by adding 0,1x sample volume of 3M NaOAc (sodium acetate) and an equivalent volume of 96% EtOH to the total volume. Samples were centrifuged and the pellets were washed with 70% EtOH. Pellets were air-dried and resuspended in 50 µl of ddH_2O. The concentration of the final DNA product was measured with Nanodrop. ddH_2O was used as a blank and the protein concentration was measured with the absorbance ratio set to 260/280 nm and 206/230 nm

The process to isolate liver DNA followed the sperm DNA isolation except that no β-mercaptoethanol was used. Liver DNA was used as positive control for PCR.

5.2.2 DNA isolation from oocyte and zygote sample

The isolation of oocyte and zygote DNA was based on the paper of Zuccotti and Monk (Zuccotti & Monk, 1995). One sample contained 10 or 20 oocytes/zygotes in 1 µl of HTF medium. Samples were resuspended in1 µl of PBS 1X, 2 µl of Proteinase K (20 mg/ml) 150X diluted and 1 µl of 15 µM SDS. Samples were incubated at 37°C for 90 minutes followed by incubation at 95°C for 15 minutes to inactivate the Proteinase K.

5.3 Analysis of DNA methylation using bisulfite sequencing

5.3.1 Principle of bisulfite sequencing

Bisulfite sequencing is a type of analytical method used to determine the methylation level of DNA. The principle of this method is a complete deamination of cytosine and its subsequent transformation to uracil. This modification is made by bisulfite, which is followed by amplification of the product using polymerase chain reaction (PCR) and sequencing. Two different sequencing methods were used: direct sequencing of the PCR product or cloning of

the PCR product and subclone sequencing. Bisulfite sequencing was developed by Frommer and his group (Frommer et al., 1992). Principle of this method is depicted in Figure 4.

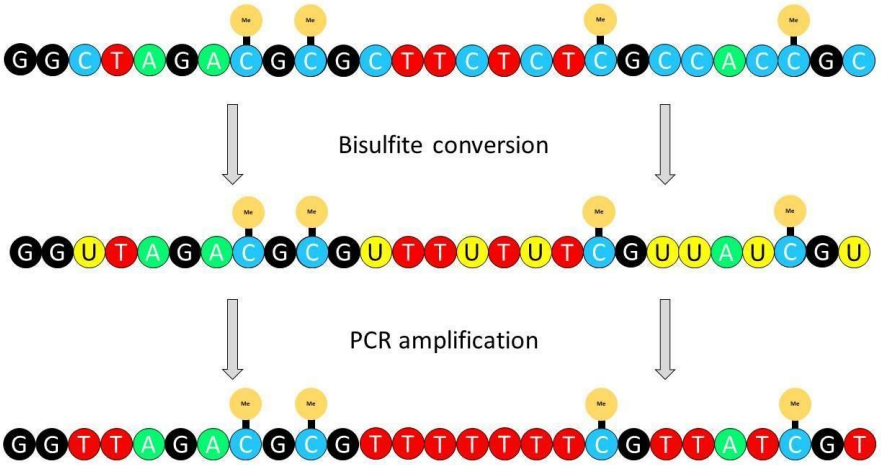

Figure 4 Scheme of two general parts of bisulfite sequencing. 5-mCs (here C with yellow circle) are not affected by the bisulfite treatment, whereas all non-methylated Cs are converted to Us. After PCR amplification, where only DNA mix of nucleotides is present, U is replaced by T. That means that all original unmethylated Cs appears as Ts at the end.

On closer inspection, the basis of this method is the reaction of bisulfite with unmethylated cytosines in a single-stranded DNA. The first step in this process is exposing DNA to an alkaline environment to obtain the single-strand DNA. Next, the C to U conversion itself takes place. This step consists of several reactions: first sulphonation, where cytosine is changed into cytosine sulphonate, second hydrolytic deamination, where cytosine sulphonate becomes uracil sulphonate, and last alkali desulphonation, where the final product of this reaction is U (Figure 5). The C to U conversion is summarised in Figure B. Originally methylated C stay unconverted. After the step of amplification using the polymerase chain reaction (PCR), all U derived from C are replaced by T. Cytosines enriched with methyl residue (5mC) stay untouched. After final sequencing, original cytosines are shown as T and 5mC appear as C.

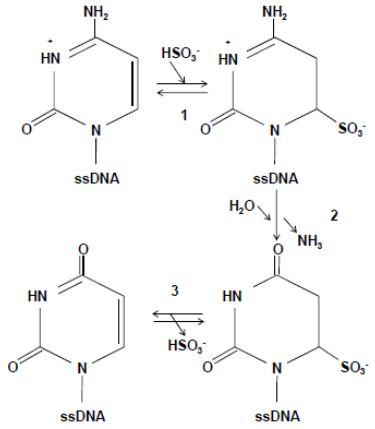

Figure 5 The chemistry of the bisulfite conversion Number 1 represents sulphonation, number 2 hydrolytic deamination and number 3 alkali desulphonation. The process begins with cytosine, followed by cytosine sulphonate, uracil sulphonate and ends with uracil. Adopted Pappas et al., 2013.

5.3.2 Bisulfite sequencing

Manufacturer's instructions for MethylEasy™ DNA Bisulfite modification kit were followed. Oocyte and sperm samples differed in the starting DNA concentrations from 20 pg up to 50 ng, and from 52 ng up to 4 ug, respectively.

Oocyte samples required immediate processing right after DNA isolation. The volume was adjusted to 10 µl with ddH_2O. Then 1,1 µl of 3M NaOH (Penta) was added to the final concentration of 0,3M NaOH and the sample was incubated at 37°C for 15 minutes. 3M NaOH was prepared fresh every time. Next, a fresh solution of sodium metabisulfite (Sigma-Aldrich) and hydroquinone (Sigma-Aldrich) was prepared. 3,3 g of metabisulfite and 3,3 mg of hydroquinone was added into 5 ml of alkaline water pH 12,9 (0,2 g of pellet NaOH into 50 ml of dH2O). After incubation with 0,3M NaOH, 110 µl of metabisulfite/hydroquinone solution was added to the sample of already denatured DNA and the sample was incubated at 80°C for 45 minutes. Then the mixture was removed into 2 ml Eppendorf tube and 2 µl of glycogen (Invitrogen) was added, followed by adding 800 µl of nuclease-free water and 1 ml of isopropanol (Penta, 67-63-0). Mixture was vortexed and incubated at 4°C for 1 hour. Sample was then centrifuged at 4°C for 15 minutes at maximal speed. The DNA pellet was washed twice in 70% ethanol for 10 minutes at maximal speed. After that, the pellet was air-dried for 15 minutes and resuspended in 15 or 20 µl of Tris-EDTA buffer. In the last step, DNA was incubated at 95°C for 30 minutes.

For sperm samples, processing right after DNA isolation was not necessary. An appropriate volume of isolated DNA was adjusted to a volume of 10 µl to obtain the amount of DNA 1 - 2 µg per sample. Following steps were the same as for the oocytes. After adding glycogen, nuclease-free water and isopropanol, samples were kept at 4°C in the fridge for 30 minutes. After that, samples were centrifuged at 4°C for 10 minutes at maximal speed. The DNA pellet was washed twice in 70% ethanol for 5 minutes at maximal speed. After that, the pellet was air dried for 15 minutes and resuspended in 50 µl of Tris-EDTA buffer. In the last step DNA was incubated at 72°C for 1 hour. The same protocol was used also for liver DNA.

5.3.3 Polymerase chain reaction (PCR)

After the bisulfite treatment, DNA was amplified using nested PCR. Primers for LINE-1 and Oct-4 were previously published (Choi et al., 2016; Lane et al., 2003), primers for Nanog were designed by Dr. Fulka. The primers are summarised in Table 1. For LINE-1, PCR conditions were 94°C for 3 min and 30 cycles of 94°C for 1 min, 56°C for 1 min, and 72°C for 1 min, followed by 10 min at 72°C (Lane et al., 2003). For Nanog and Oct-4, PCR conditions were identical, specifically 94°C for 3 min and 35 cycles of 94°C for 1 min, 52°C for 1 min, and 72°C for 1 min, followed by 10 min at 72°C.

Name of product	**Forward primer** **Reverse primer**	**Length of product**	**Accession number/ position**
LINE–1 5´external	TAGGAAATTAGTTTGAATAGGTGAGAGGGT	299	D84391.1
	CCAAAACAAAACCTTTCTCAAACACTATAT		
LINE–1 5´ internal	GTTAGAGAATTTGATAGTTTTTGGAATAGG	250	
	TCAAACACTATATTACTTTAACAATTCCCA		
Nanog external	GTATTATAATGTTTATGGTGGATTTTGT	324	CH6 122704489 - 122716633
	AACAACAACCAAAAAACTCAATATCTA		
Nanog internal	TTTATGGTGGATTTTGTAGGTGG	215	
	CAACCTTCCCACAAAAAAAACAAA		

Oct–4 external	GGGATTTTTAGATTGGGTTTAGAAAA	283	CH17 35501450 - 35536729
	ACTCCCCTAAAAACAACTTCCTACT		
Oct–4 internal	AGGGTAGGTTTTTTGTATTTTTTTT	157	
	CTCCTCAAAAACAAAACCTCAAATA		

Table 1 The list of primers used in the PCR reactions

DNA was amplified using Taq DNA Polymerase (High QU, PCE0202). First round PCR, DNA was amplified in 20 µl reaction volume, second round was increased to 50 µl of reaction volume. The components of the reaction mixture were as follows:

Nanog / Oct-4

First run

- 14,45 µl nuclease free H_2O
- 2 µl 10X PCR Buffer (High QU)
- 1,2 µl 50 mM $MgCl_2$ (High QU)
- 0,25 µl dNTPs 20mM each (Solis BioDyne)
- 1 µl mix of primers, 10 µM each
- 0,1 µl Taq DNA Polymerase (High QU)
- 1 µl template (BS DNA)
- 20 µl TOTAL

Second run

- 38,4 µl nuclease free H_2O
- 5 µl 10X PCR Buffer (High QU)
- 3 µl 50 mM $MgCl_2$ (High QU)
- 0,6 µl dNTPs 20mM each (Solis BioDyne)
- 1,5 µl mix of primers, 10 µM each
- 0,5 µl Taq DNA Polymerase (High QU)
- 1 µl template (first reaction)
- 50 µl TOTAL

LINE-1

First run

- 14,85 µl nuclease free H_2O
- 2 µl 10X PCR Buffer (High QU)
- 0,8 µl 50 mM $MgCl_2$ (High QU)
- 0,25 µl dNTPs 20mM each (Solis BioDyne)
- 1 µl mix of primers, 10 µM each
- 0,1 µl Taq DNA Polymerase (high QU)
- 1 µl template (BS DNA)
- 20 µl TOTAL

Second run

- 39,9 µl nuclease free H_2O
- 5 µl 10X PCR Buffer (High QU)
- 2 µl 50 mM $MgCl_2$ (High QU)
- 0,6 µl dNTPs 20mM each (Solis BioDyne)
- 1,5 µl mix of primers, 10 µM each
- 0,5 µl Taq DNA Polymerase (High QU)
- 0,5 µl template (first reaction)
- 50 µl TOTAL

Amplified DNA was detected on 2% agarose gel. 10 µl of PCR reaction was mixed with 2 µl 6X MassRuler Loading Dye (Fermentas). Agarose gel was prepared of 2 g of agarose powder (SERVA, CAS 9012-36-6) and 0,5% TBE buffer (Merck), volume up to 100 ml. After boiling, 5 µl of Midori Green Advance DNA Stain (Genetics) was added to the liquid agarose mixture.

If the DNA product from the bisulfite conversion step was resuspended in the optimal volume of the TE buffer, only some PCR showed the result. This was the proof that single molecules of converted DNA were picked for the PCR reaction.

5.3.4 Sample sequencing

Samples of amplified BS DNA were sent off to company Seqme s. r. o. for external sequencing. By testing, particular primers were chosen for each type of sequence. Samples for sequencing were prepared as follows: 0,5 – 1 µl of PRC reaction adjusted to 5 µl with nuclease-free water mixed with 5 µl of 5 µM primer suitable for the PCR product.

5.4 Analysis of protein lamin A/C in GV oocyte

To find out what the amount of protein Lamin A/C is per one GV oocyte, the SDS-PAGE and Western blot methods were used.

5.4.1 Standard curve

As a tool for obtaining the information about protein concentration a standard curve was used. The standard curve is used for determining the relationship between absorbance and protein concentration. The samples of known concentration are called standards. When the values of the absorbance are collected from the standards, the relationship between absorbance and the protein concentration can be drawn as a graph. This is called a standard curve. The equation describing the graph is used to determine the unknown concentration of the protein of the interest. Here, the recombinant protein Lamin A/C was used (Cloud-Clone Corp, RPF550Mu01). Lyophilised protein was reconstituted according to the protocol (see chpt. Material) to a final concentration of 0,5 mg/ml. Protein was aliquoted and stored at -80°C.

For the standard curve, eight descending protein concentrations were prepared with the same buffer that was used for its reconstitution. The concentration of each sample was as followed: 50 ng/µl, 20 ng/µl, 8 ng/µl, 3,2 ng/µl, 1,28 ng/µl, 0,512 ng/µl, 0,204 ng/µl, 0,081 ng/µl (Figure 6). The volume of each sample was 3 µl. In the first tube the volume of 5 µl containing 50 ng/µl was prepared. Next, 7 tubes with 3 µl of buffer were prepared. 2 µl of solution was taken from the first tube and put into the second tube and mixed well. This process continued until reaching the last tube.

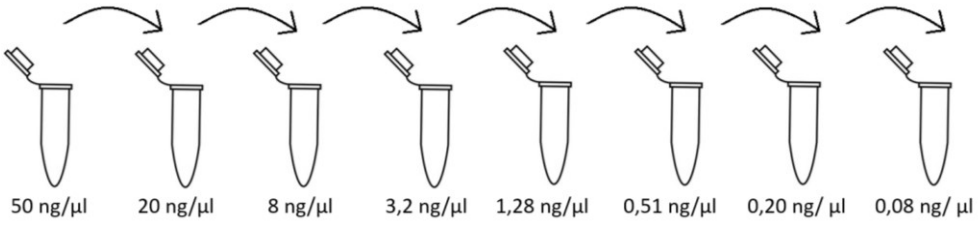

Figure 6 Description on serial dilution in purpose to create standard curve

5.4.2 SDS-PAGE

The samples contained a different number of GVs (from 20 to 60 GVs). After GV isolation in HTF medium, GVs were washed in 0,1% PVA (polyvinylalcohol) in 1X PBS buffer and collected in a drop of 2,5 µl of this buffer and stored in - 80°C until further use. Mouse pulmonary tissue was used as a positive control. 50 mg of a lung was cut off. The lysis buffer was made of 890 µl of H2O, 100 µl of 10X RIPA buffer (TermoFisher) and 10 µl of inhibitor solution (SERVA). 500 µl of lysis buffer was added to the tissue. The tissue was minced, followed by a centrifuge at 4°C for 20 minutes, 15 000g.

Prepared samples were mixed with Laemmli sample buffer (Bio-Rad) with 5% β-mercaptoethanol (Sigma) in a1:1 ratio and boiled at 95°C for 5 minutes. After that, the samples were loaded on the acrylamide gel. For the SDS-page, 10% acrylamide gel was prepared (Bio-Rad). The maximum volume of each sample was 5 µl. The SDS-page construction was set up (Bio-Rad). Gel was run in Tris-Glycine-SDS 0,1% buffer (see chpt. Materials) under the current of 15 mA per one gel for about an hour.

5.4.3 Western blot

Transfer: Following a successful SDS-PAGE, PVDF membrane (Cytiva Amersham™) was used for the protein transfer. The membrane was activated by methanol wash for 10 seconds and Towbin buffer wash (see chpt. Materials). The gel and the membrane were put into the transferring cassette. Electro-transfer went under cooling conditions at 46V, 360 mA for 4 hours in the Towbin buffer. The membrane was then quickly washed in distilled water and air-dried at 37°C for 1 hour.

Blocking: The dried membrane was reactivated by washing in methanol for 10 seconds followed by washing in TBST 0,05% (see chpt. Materials) for 5 minutes. The 3% blocking

solution was prepared from 1,5 g of ECL Advance™ blocking agent (Amersham™) and 50 ml of TBST 0,05%. In this solution, the membrane was incubated at room temperature for one hour, shaking. After that, the membrane was washed three times in TBST 0.05%, each wash 5 minutes.

Primary antibody: For Lamin A/C detection, the rabbit polyclonal primary antibody (Santa Cruiz) was used. The antibody was diluted in the blocking solution at 1:5000 ratio. The membrane was incubated in the primary antibody in a cold room overnight, typically 20 hours, while shaking.

Secondary antibody: As secondary antibody the goat anti-rabbit antibody was chosen (Abcam). After overnight incubation in the primary antibody, the membrane was washed four times in TBST 0.05%, each wash 5 minutes. The secondary antibody was diluted in TBST 0.05% at 1:100 000 ratio. After washing, the membrane was incubated in the secondary antibody at room temperature for one hour, shaking. Afterwards, the membrane was washed three times TBST 0,05%.

For visualising the bands on the membrane, the substrate ECL Select (Cytiva Amersham ™) was used. The Peroxide solution and the Luminol solution were mixed together in a 1:1 ratio and 250 – 300 µl was spread on the membrane. The detection was done with Aruze c300. Exposure time was set to 3 minutes.

5.5 In vitro fertilization (IVF)

IVF followed the protocol from Harwell Institute based on the work published by Takeo et al. (Takeo & Nakagata, 2011). For MII oocytes collection, the same mouse stimulation was performed as described above. On the day of IVF, two dishes were prepared. First, the sperm dish: 200 µl of TYH medium was dropped into a dish and covered with mineral oil. The drop was ellipse shaped. The dish was equilibrated at 37°C, 5% CO_2 in the incubator for 10 – 20 minutes. Second, the fertilization dish. The main stock of 25 mM reduced glutathione (GSH) in HTF was prepared. From this stock, 12,5 µl was pipetted into a new Eppendorf tube and filled up with HTF to the volume 500 µl to final concentration 0,625 mM. 200 µl of 0,625 mM GSH medium was dropped into a dish. Next to the drop, 5 drops of 90 µl of KSOM medium were dropped into the same dish and covered with mineral oil. The dish was equilibrated at 37°C, 5% CO_2 in the incubator for up to one hour.

The sperm for the IVF was obtained the same way as described above. The sperm was allowed to disperse throughout the drop for 1 hour at 37°C, 5% CO_2 in the incubator. For obtaining the MII oocytes, the oviducts were transferred into the mineral oil. The swollen ampullas were gently cut and COCs were released into the oil. Then the COCs were removed to the drop of fertilization medium. The dish with COCs was equilibrated at 37°C, 5% CO_2 in the incubator for 30 minutes.

Finally, 12 µl of dispersed sperm was added to the fertilization dish with COCs. The dish was placed back to the incubator for approximately 3-4 hours to allow fertilization to occur. Then the presumptive zygotes were removed to the first drop of KSOM medium and washed in each KSOM drop. The dish was put back to the incubator for appropriate time depending on the following processes.

5.6 Removing the nucleus of the cell

For obtaining the cell without the whole nucleus or without part of the nucleus, the micromanipulation methods selective enucleation (SE) and complete enucleation (CE) were chosen. These methods were done by Mgr. Helena Fulka, Ph.D. The principle of SE is removal of insoluble nuclear fraction, while the soluble nuclear fraction is left behind and the soluble fraction is spread into the cytoplast. Nucleoli also remain in the cytoplast. The insoluble fraction is removed by fine pipette, while the holding pipette keeps the oocyte at one position with negative pressure. SE was used for GV oocytes.

CE is removing the whole nucleus using the same mechanisms. This method was used for MII oocytes.

6 Results

6.1 Obtaining DNA from gametes and zygotes

To elucidate the change of methylation before and after fertilization, the single gametes, oocytes and sperm, and zygotes were used. First, DNA had to be isolated.

In the case of the sperm, DNA was isolated using a lysis buffer with Proteinase K and β-mercaptoethanol and purified with phenol-chloroform precipitation. The pellet was

resuspended typically in 30 µl of ddH_2O and the concentration was measured using Nanodrop 3000. Approximately 120 – 200 ng/µl was isolated from each sample. The ratio of absorbance at 260 nm and 280 nm was around 1,8 and the ratio of absorbance at 260 nm and 230 nm was around 2,1. Isolated DNA was stored at -20°C. The isolated sperm DNA was tested to be stable for up to three months.

In the same manner, DNA from the spleen was isolated and purified. The spleen DNA was used as a positive control in the PCR. The spleen tissue was used due to simple manipulation and big dosage of DNA.

Compared to sperm, only a small number of oocytes or zygotes was available. DNA was typically isolated from the samples containing from 15 to 20 MII oocytes or zygotes. No lysis buffer was used. DNA was isolated with a solution of Proteinase K, 15 µM SDS and 1X PBS (see chpt. Methods). Isolated DNA was always directly used for bisulfite sequencing without measuring the concentration or purity on Nanodrop.

6.2 Elucidating the DNA methylation level

The protocol for bisulfite conversion was modified depending on the DNA input amount. The protocol distinguished between the amount up to 50 ng, used for MII oocytes and zygotes, and the amount from 51 ng up to 4 µg, used for sperm. Converted DNA was precipitated, and the pellet was resuspended in the Tris-EDTA buffer. MII oocyte and zygote modified DNA (BS DNA) pellets were typically resuspended in 20 µl of buffer, whereas the sperm modified DNA pellet in 50 µl of buffer. BS DNA was used as a template for PCR. The amplification step was important for increasing the signal, because during bisulfite conversion approximately 90% of DNA is degraded.

Gene promoter of Nanog (213 bp) and Oct-4 (157 bp) proximal enhancer (PE) are typically used as model for examination of active demethylation. For PCR, primers corresponding to these DNA sequences were chosen based on the literature. The aim for the PCR was to amplify a single molecule of DNA. For obtaining this result, BS DNA template has to be diluted appropriately. Several PCR reactions were prepared for the same template and the same group of primers. The outcome with some positive and some negative results was desired (Figure 7). This outcome was the proof that the BD DNA template was diluted

correctly, and single molecules were caught for certain PCR reactions. Positive reactions were sent to a sequencing company Seqme.

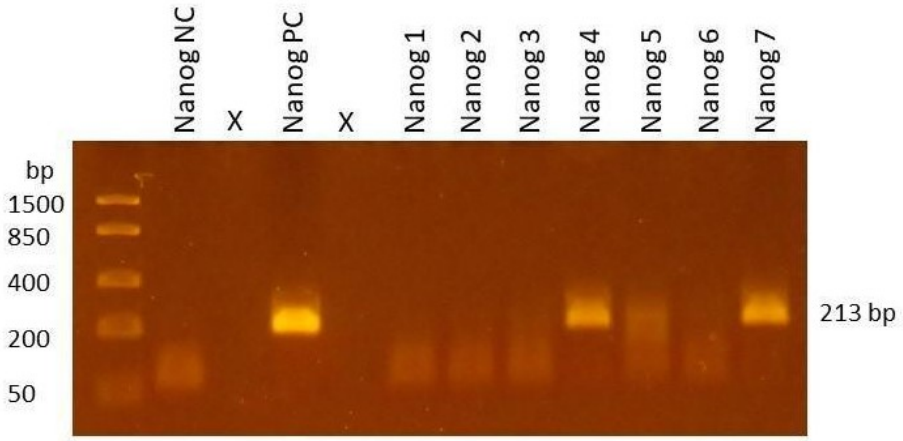

Figure 7 Example of agarose gel of PCR reaction. Master mix with Nanog primers was prepared for nine reactions in total. One reaction was used as negative control (NC) with no template. Another reaction was used as a positive control (PC) with BS DNA from the spleen as a template. Next, seven reactions were used for BS DNA from gametes or zygotes. BS DNA template had to be diluted appropriately. In this case, PCR reactions Nanog 4, Nanog 5 and Nanog 7 were sent for sequencing.

The data obtained from Seqme company were compared with a model methylation of sequences using software BioEdit. Form of a model methylation of sequences was prepared manually using Microsoft Word. The sequencing results were compared with literature. Both processes are summarised in Figure 8.

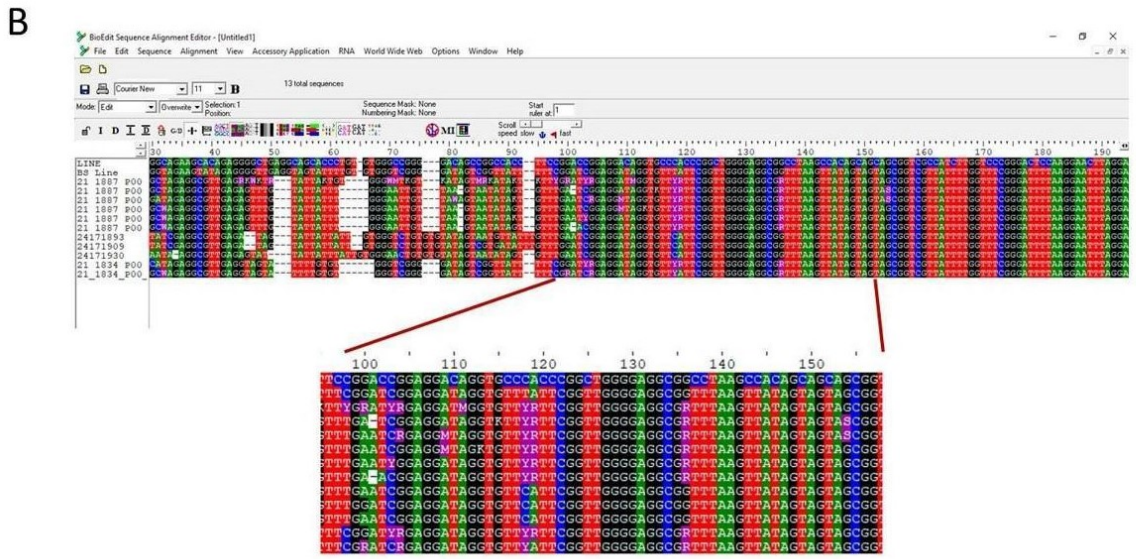

Figure 8 Comparing results from sequencing to model methylation. A) Hand-made conversion. First step: All CG were replaced by XY, representing methylated dinucleotides. Second step: All C were replaced by T, representing BS conversion. Last step: All XY replaced back by CG. The last picture represents DNA sequence after BS conversion with methylated CG. B) Illustration of comparison of sequencing results and model methylation using BioEdit software. First lane in untreated sequence with all original C. Second lane is model methylation. The rest represents sequencing results of PCR reactions.

6.2.1 The DNA methylation level before fertilization

The DNA methylation of single gametes was verified. The DNA methylation level in sperm was higher than the DNA methylation level in MII oocytes. Both Nanog and Oct-4 were hypermethylated in sperm but in MII oocytes, Oct-4 was more methylated than Nanog (Figure 9). The obtained data are in accordance with the literature.

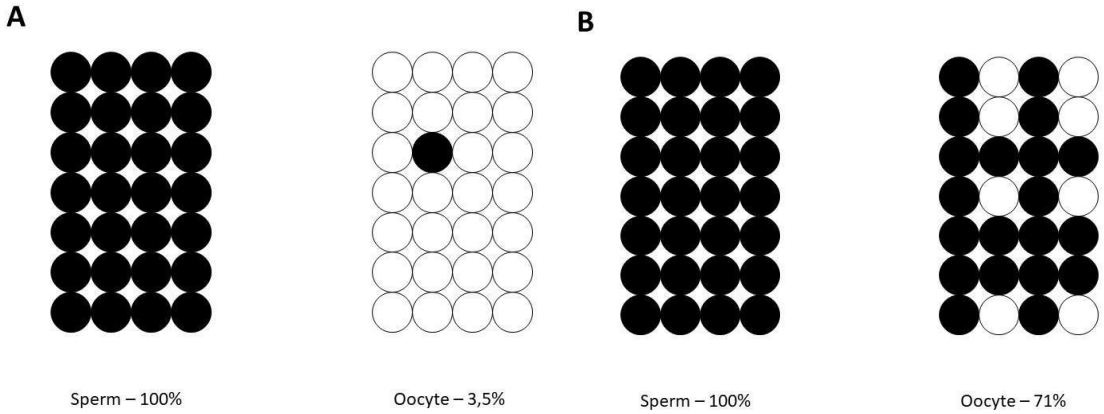

Figure 9 CpG methylation level in chosen sequences in sperm and oocytes. Circles represent CpG pairs, black = methylated, white = unmethylated. Each line represents one PCR reaction. (A) Nanog promoter sequence containing 4 CpG pairs. For sperm, all Nanog CpGs were methylated. On the other hand, Nanog in oocytes is almost demethylated. (B) Oct-4 PE sequence containing 4 CpG pairs. For sperm, the situation is the same as with Nanog. But the sequence in oocytes is more methylated than Nanog.

6.2.2 The DNA methylation level after fertilization

Zygote DNA methylation was elucidated and different results were obtained in comparison with gametes. In both cases of Oct-4 and Nanog, the decrease of DNA methylation was observed (Figure 10). Data proved that there is a change in methylation right after fertilization and the result also confirmed that both regions of Oct-4 and Nanog are demethylated actively (Figure 11). The obtained data are in accordance with the literature.

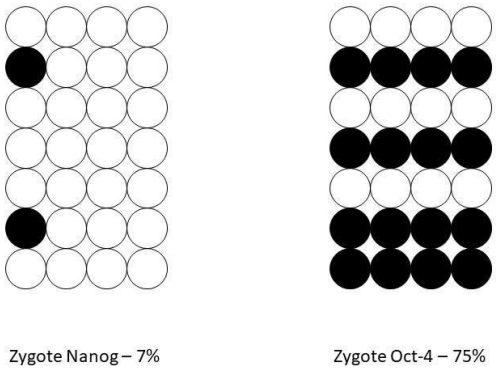

Figure 10 CpG methylation level in chosen sequences in zygote. Circles represent CpG pairs, black = methylated, white = unmethylated. Each line represents one PCR reaction. After fertilization, Nanog is more demethylated.

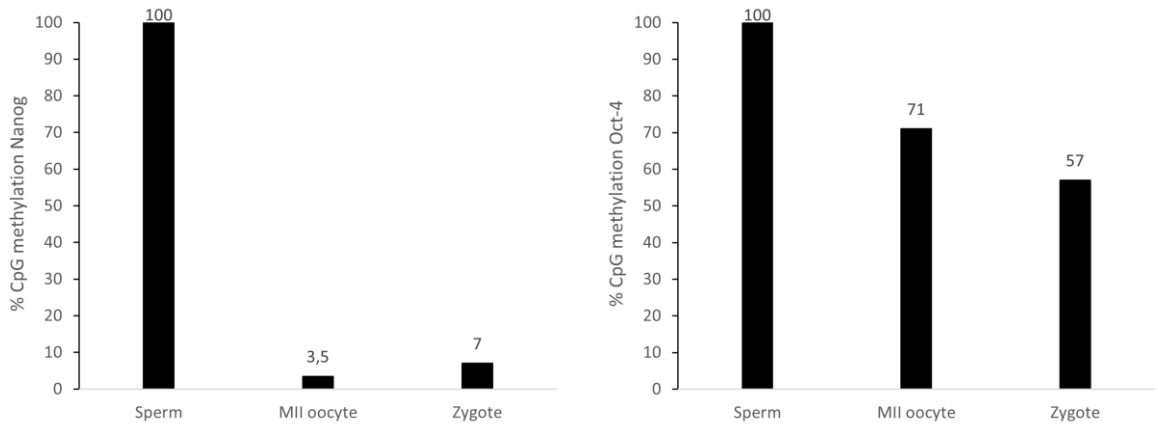

Figure 11 Comparison of Nanog and Oct-4 methylation level in sperm, MII oocyte and zygote. Graphs are showing the level of CpG methylation of Nanog and Oct-4, comparing the level before and after fertilization. In the case of Nanog, there is an obvious decrease of methylation in zygotes, Oct-4 sequence methylation also decreased visibly.

6.3 Determination of the amount of lamin A/C in GV oocyte

To determine the amount of protein lamin A/C in one GV oocyte, methods SDS-PAGE and Western blot were used. Prepared samples of oocytes contained from 24 up to 56 GV oocytes in 2,5 – 3,5 µl PBS with 0,1% PVA. For SDS-PAGE, due to a small volume of samples, Laemmli

sample buffer was added directly to the GV sample. In contrast, lung tissue, used as a positive control, was minced in RIPA buffer with protease inhibitors and centrifuged before adding Laemmli sample buffer.

In the final step, from all experiments five WB membranes were chosen for analysis. Pictures of prepared WB membranes were taken by Azure imaging system (Figure 12) The molecular mass of recombinant protein is 52kDa and the molecular mass of lamin A/C is 65kDa.

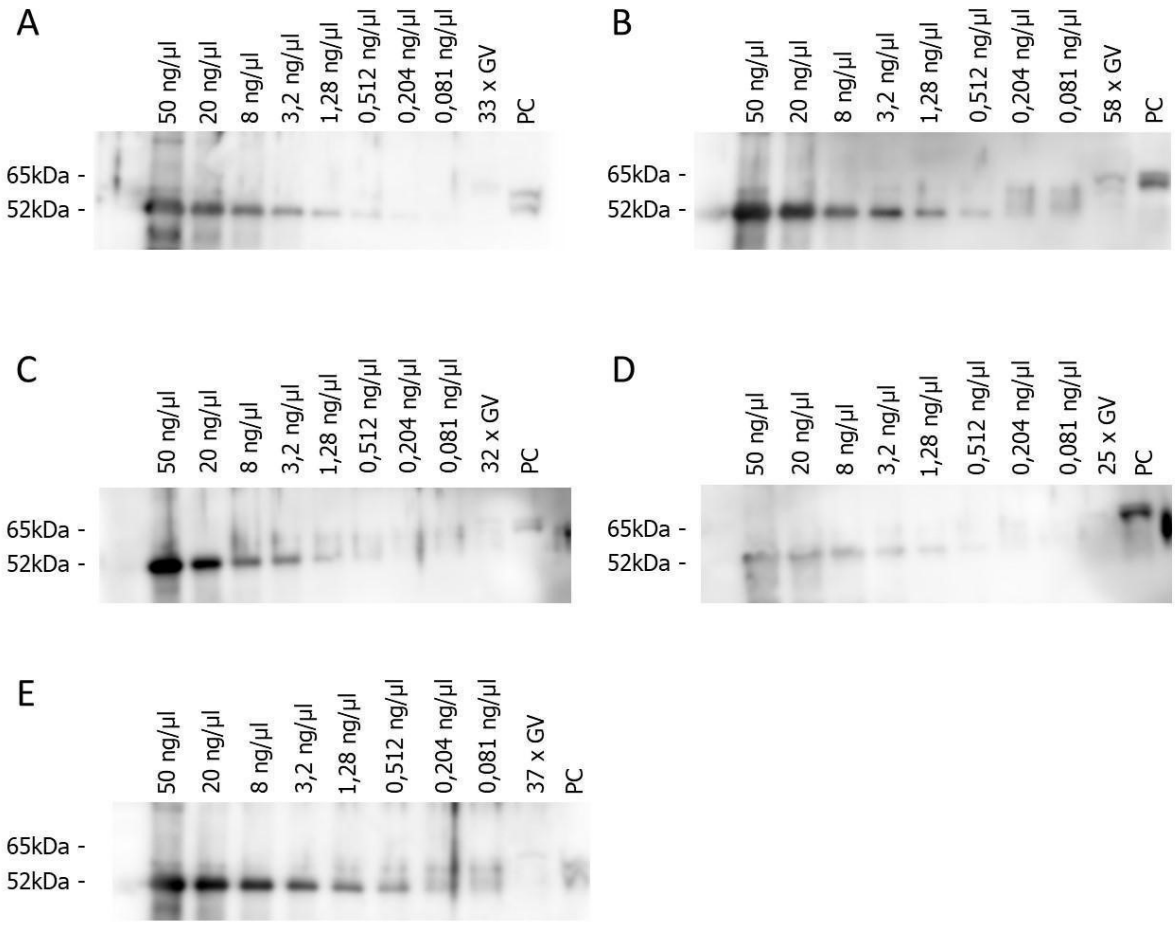

Figure 12 Western Blot analysis of standard curve of recombinant protein lamin A/C and lamin A/C in GV. The dilution row of recombinant protein lamin A/C was prepared. Each sample of known protein concentration was loaded into the wells of the SDS-PAGE gel. In each experiment, different amounts of GV were used: A – 33 GVs, B – 58 GVs, C – 32 GVs, D – 25 GVs, E – 37 GVs. Lung tissue was used as positive control (PC).

After membrane shooting, pictures were analysed in software Fiji programme ImageJ. The determination of protein amount was done by using a standard curve. The intensity of each band signal and background signal was measured and noted to the programme Microsoft Office Excel. Each band of the standard curve represented a known concentration of

recombinant protein lamin A/C in sample volume 2,5 µl. Based on the known protein concentration, volume of samples and band signal intensity, the graph with the trendline was calculated using Microsoft Office Excel. A background signal was taken into consideration from each band signal. The graph equation was generated. Using this equation, it was possible to calculate the concentration of GV samples. GV sample band intensity was measured the same way as standard curve bands intensity. All graphs and corresponding equations are summarised in Figure 13.

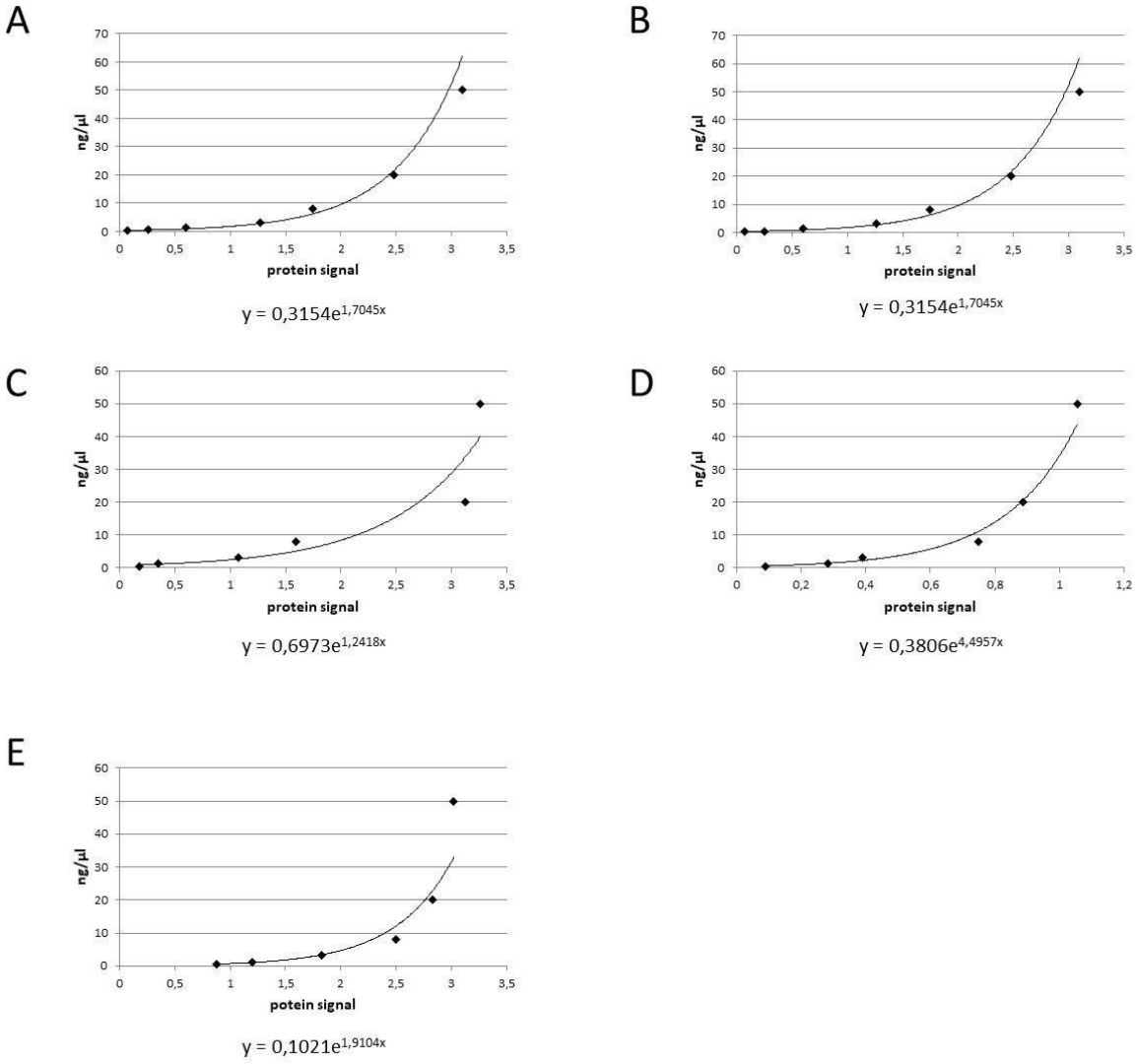

Figure 13 Western blot results. A-E Graphs created in the program Microsoft Office Excel. Each graph corresponds to a single membrane. The relationship between protein concentration and signal intensity is depicted. The corresponding equations are below the graphs. These equations were used to count the protein concentration in each GV sample.

n GV	Background	Protein signal	Background adjusted protein signal	ng/µl	V (µl)	m (ng)	1 x GV (pg)
33	0,423	0,558	0,135	0,397	2,5	0,993	30,08
58	0,423	0,558	0,135	0,397	3	1,191	20,53
32	0,805	0,572	0,233	0,931	3	2,794	87,31
25	0,79	0,559	0,231	1,075	2,5	2,688	107,52
37	0,212	0,397	0,185	0,145	3	0,436	11,79
Average							51,45

Table 2 Table summarizing the results for each GV sample. The background signal was subtracted from each band signal. Protein concentration(ng/µl) for each GV sample was calculated using equations generated the program Microsoft Office Excel.

Using the average of all five membranes, the amount of protein lamin A/C was determined to be 51, 45 pg per one oocyte (Table 2). The amount (ng) of protein lamin A/C was calculated by multiplying the sample volume (µl) and the protein concentration (ng/µl). The result was divided by the number of GV in corresponding sample.

6.4 The DNA methylation in androgenetic embryos and SE embryos

This experiment was carried out by the supervisor of this thesis, Mgr. Helena Fulka, Ph.D. and her colleague, Bc. Zuzana Smékalová. In the main experiment, GV oocytes were rid of the nuclear envelope by the method selective enucleation. Using this method, the insoluble fraction of GV (e.g. nuclear envelope, nuclear lamina, chromatin bound proteins etc.) can be removed and the soluble fraction stays distributed in the cytoplasm of the oocyte. An appropriate amount of the recombinant protein lamin A/C was supposed to be microinjected into these oocytes. The result of the micromanipulation experiment would have been a GV oocyte without the insoluble fraction of GV, although obtaining protein lamin A/C, which is the part of the nuclear lamina. These oocytes would have been fertilized by IVF. IVF would have been followed by the same procedure as single oocyte or zygotes. The DNA would have been isolated first, then the bisulfite sequencing would have been performed. The result could have answered the question, if the lamin A/C has an impact on active DNA demethylation of the paternal pronucleus after fertilization.

Because of the lack of time due to a long optimization time and unsuitable PCR results, the final experiment was not carried out. To complete the aim of this study, an alternative experiment was designed.

For bisulfite sequencing, three types of samples were prepared. First, zygotes prepared by standard IVF, which were used as positive control. Second, one-cell embryos, which were prepared by SE of GVs followed by their IVF. These samples served as a negative control. Third, androgenetic embryos, which were prepared by complete enucleation of MII oocytes followed by their fertilization using IVF. These samples were supposed to substitute SE-samples with microinjected recombinant lamin A/C from the original experiment (Figure 14).

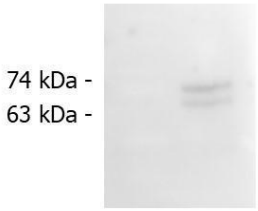

Figure 14 Confirmation of presence of lamin A/C in MII cytoplast. This WB membrane was prepared by Bc. Zuzana Smékalová. After GVBD, MIIs contain lamin A/C spread in thecytoplast. Removal of insoluble chromatin and bound proteins does not have any impacts. Sample: 70 cytoplasts Lamin A/C (4C11, 4777) Mouse mAb Cell Signalling – 74 kDa lamin A, 63 kDa lamin C

The protocol of elucidation of the DNA methylation was the same as for MII oocytes or in vivo zygotes. First the process of DNA isolation was done by solution of Proteinase, 15 µM SDS and 1X PBS (see chpt. Methods), followed by the bisulfite conversion. BS DNA was used as a template for the PCR. The same area of Nanog and Oct-4 PE were analysed. Positive PCR reactions were sent for sequencing and the results were compared with model methylation of sequences. All results are depicted in Figure 15.

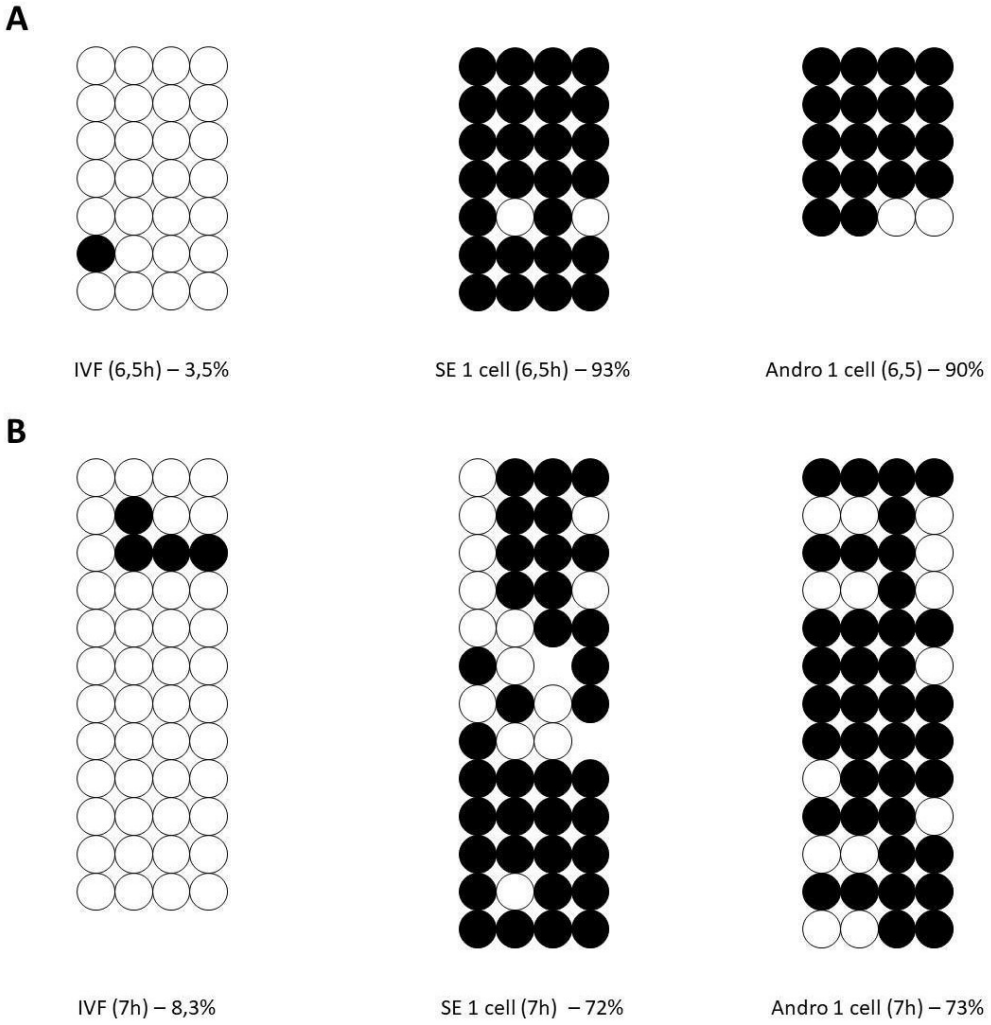

Figure 15 CpG methylation level in androgenetic embryos. Circles represent CpG pairs, black = methylated, white = unmethylated. The gap represents inappropriately sequenced CpG pair. Each line represents one PCR reaction. Numbers in brackets represent hours post fertilization. (A) Nanog promoter sequence containing 4 CpG pairs. (B) Oct-4 PE sequence containing 4 CpG pairs. The situation in Nanog is like the one in Oct-4 PE.

The IVF positive control proved that the active demethylation occurs prior to 8 hours post fertilization. This is in correlation with literature. On the other hand, SE control proved that the active demethylation does not proceed without the insoluble fraction of GV. The methylation level is similar to the methylation level before fertilization (Figure 9). The results of androgenetic embryos showed that there is no active demethylation (Figure 15). The result was very similar to the results of SE embryos. The difference between SE and androgenetic embryos is the presence of maternal lamin A/C. Obviously, lamin A/C does not have any impact on the demethylation after fertilization.

To sum up, these results lead to a suggestion that the insoluble fraction of GV has an essential role in the active demethylation of the paternal genome. However, it is still not clear, which component or components have the main impact.

7 Discussion

The aim of this study was testing the hypothesis that the components of insoluble GV fraction are necessary for paternal genome formation and securing the proper embryonic development. We hypothesized that the insoluble GV fraction would contain a factor/factors that are necessary for a full functionality in development. More specifically, this work tried to outline the role of insoluble GV components in active DNA demethylation after fertilization. We focused on the role of lamin A/C, a part of insoluble fraction, and its role in initiation of BER, which can remove oxidized form of 5mC, which is the methylation mark.

After fertilization, the paternal genome undergoes a massive loss of DNA methylation. Because the first rapid process, which is completed after fertilization, is protamine to histone transition, it was originally thought that the active DNA demethylation was achieved by remodelling of sperm chromatins (S. H. Kim et al., 2004). Nowadays, a lot of studies support the idea that the main loss of methylation is caused by changing the chemistry of 5mC. The genome-wide DNA demethylation is mainly mediated by maternal TET3s, which oxidize 5mC to create 5hmC. The oxidation reactions continue with 5fC and 5caC. Nevertheless, this proposed mechanism is starting to be challenged.

5hmC starts to appear during the late zygotic stage at PN4, predominantly in the paternal pronucleus in zygote. However, the 5mC level decreases by the early PN3 stage. Also, there is not an equal correlation between the total amount of 5hmC and the level of 5mC loss, the level of 5hmC is lower than the level of 5mC loss. This all points to the situation that there is not a continuous transition from 5mC to 5hmC (Santos et al., 2013). Moreover, 5fC and 5caC do not come out gradually after 5hmC, but they appear concomitantly with 5hmC (Inoue et al., 2011). Also, it was detected that the generation of 5fC takes place from PN3 until PN5. These together lead to the suggestion that the active DNA demethylation by TET3 enzymes occurs at later zygotic stages and not right after fertilization (C. Zhu et al., 2017). At PN4 and PN5 approximately 70% of the paternal 5mC is lost when compared to the sperm (Amouroux et al., 2016).

Maternal TET3s play an important role in oxidation of 5mC in paternal pronucleus and the loss of TET3s leads to decrease of 5mC oxidised forms. Nevertheless, the absence of TET3s or the blocking of their function probably does not have any impact on the initial loss of paternal 5mC in the early PN3 stage. However, the lack of 5hmC formation is still present in

the paternal pronucleus. In conclusion, the 5hmC is not demanded for major zygotic 5mC removal in early PN3. The loss of 5mC and the formation of 5hmC are to some extent two independent processes and TET3 knockout has only limited effect on zygotic DNA demethylation (Amouroux et al., 2016). This evidently opens the field for other possibilities as to how paternal 5mC could be lost in such a short time after fertilization.

Because the oxidation of DNA is classified as a damage, the repair mechanisms should be considered as an important participant in the demethylation process. One of the most common DNA lesions resulting from oxidation damage is 8-oxoG (Kanvah et al., 2010), which is normally repaired by the BER pathway (Whitaker et al., 2017). Moreover, it was even suggested by authors that single strand DNA breaks occur after fertilization and the repair pathway BER takes part in active demethylation as well (Hajkova et al., 2010; Wossidlo et al., 2010). BER could be induced by DNA lesions, which could be caused by DNA glycosylases. These enzymes recognize mismatches in DNA strands and they create nicks by removing the inappropriate bases. An example of DNA glycosylase is TDG, which is able to remove oxidized forms of 5mC and initiate BER. 5fC and 5caC could easily be recognized as 5mC by TDG and removed. However, these oxidized forms of 5mC occur at later PN stages. If BER participates in active demethylation, it must be initiated by some other factors. One suggestion is brought by Maynard et al., who suggested that BER could be promoted by lamin A/C (Maynard et al., 2019). This would be interesting for this thesis, because lamin A/C is a part of insoluble GV fraction, which is the subject of investigation. The question arose: does lamin A/C have indirect influence on BER by influencing the level of gene expression of the BER components as described Maynard et al.? Or does lamin A/C have any other general or specific impact on BER, e.g. 8-oxoG repair?

In the first part of the project, the methylation level of DNA sequences was verified. For this verification, sequences of Nanog and Oct-4 promoters were chosen. These genes are typically used for studying dynamics of epigenetic reprogramming in preimplantation embryos (Al-Khtib et al., 2012; Tsai et al., 2012; Wang et al., 2009; Zhao et al., 2013). These genes are also good models because they belong to the group of genes which are necessary for pluripotency and early embryonic development (G. Wu & Schöler, 2014). Promoters in active mammal genes are typically demethylated in CpG dinucleotides (Weber et al., 2007). Therefore, for a quick activation of these genes the active DNA demethylation is necessary.

This is also a reason as to why Nanog and Oct-4 are plentifully used in active demethylation studies (Choi et al., 2016; Farthing et al., 2008).

Originally, the methods were planned for LINE-1 sequences. LINE-1 carried a lot of opportunities for studying genome methylation level, since it was shown the DNA methylation level of LINE-1 is lost during zygotic reprogramming (Lane et al., 2003). In the case of this thesis, LINE-1s were interesting sequences, because it was even proved that the LINE-1 sequences are associated with protein lamin A/C in nuclear lamina (Vazquez et al., 2019). Even though DNA demethylation in paternal pronucleus is predominantly active and replication-independent process, LINE-1s belong to the group of sequences where DNA demethylation happens gradually and it is lost through passive demethylation and it relies on the correct completion of S-phase (Guo et al., 2014).

Our results confirmed that the methylation level is lost after fertilization (Figure 11). The level of methylation was higher in gametes than in zygotes, as expected. In both gene promoters the methylation was higher in sperm compared to MII oocytes. This is in accordance with the literature (Donkin & Barrès, 2018; Kobayashi et al., 2012).

The methylation level after fertilization is not the same for Nanog and Oct-4. One of the reasons is the fact that DNA for BS was isolated from zygotes obtained in vivo. The zygotes did not have to be isolated at the same time after mating. Hence, there could be different levels of DNA demethylation. However, it is important that in both Nanog and Oct-4 the obvious demethylation was observed. Moreover, compared to the literature, (Choi et al., 2016) Oct-4 shows higher levels of methylation than Nanog after fertilization. This evidence supports our results.

Bisulfite sequencing used in this study is not the most suitable method for DNA methylation level detection, because this method cannot distinguish between 5mC and 5hmC. (Booth et al., 2013). However, the increase of 5hmC was observed after the main decrease of 5mC and independently on the DNA replication (Santos et al., 2013). In the case of this study, the DNA from androgenetic embryos was analysed prior to 7 hours post fertilization, which should be before the first replication. Hence, bisulfite sequencing is sufficient in this case

The main experiment of this project was inspired by the work of Maynard et al. and his colleagues (Maynard et al., 2019). In their work they investigated the protein lamin A/C as the initiator of the repair mechanism BER. As it was described before, BER is more or less another step in the DNA demethylation pathway after oxidation of 5mC by TET3 enzymes. Next to work

of Maynard et al. it has been also proposed that the active DNA demethylation after fertilization is putatively accompanied by the appearance of DNA strand breaks and it is connected to the DNA damage repair (Hajkova et al., 2010; Wossidlo et al., 2010).

Typically, BER is induced at first by ssDNA lesions. These lesions are created by e. g. glycosylases, such as TDG. TDG is able to recognize mismatches in DNA and deplete inappropriate bases (Neddermann et al., 1996). Another enzyme inducing the BER is AID. This enzyme was proposed to be a part of the active demethylation in zygotes and also the following BER pathway (Santos et al., 2013). But the work of Maynard et al. points to the new putative player. It has been demonstrated that depletion of lamin A/C has a negative impact on the mechanism connected to BER activity and decreases the expression of some BER components. It is important to remember that Maynard and his colleagues performed the process on cell lines, namely MEF and U2OS cells. The big disadvantage of cell lines is that the cells have active gene expression, hence this system can investigate only the indirect impact of lamin A/C depletion and its effect on the expression of the BER components. The exposure of the cells to the stress surroundings might have an impact on the gene expression and can lead to the change of physiological characteristics.

The aim of this project was to challenge Maynard's work and try whether the work is suitable for other cell types in the natural environment. Their work was designed for investigating the indirect influence of lamin A/C on BER, because they focused on the gene expression of BRE components in cell lines, where the gene expression is running. We wanted to test the direct influence of lamin A/C on BER. For that, we needed a system without gene expression. It was planned to utilize GV oocytes as model cells. For verification of the role of lamin A/C in BER, GV oocytes could serve as a good model because there is no gene expression in these cell types. A depletion of any protein cannot have any impact on the regulatory networks or the level of any kind of mRNAs. The same is true for zygotes.

Lamin A/C, as a part of nuclear lamina, belongs to the insoluble fraction of GV. It has been previously proposed in unpublished studies that the soluble fraction of GV is essential for male pronucleus formation and a successful sperm head remodelling. Interestingly, nuclear membrane is dispensable in these processes. However, for reaching the full developmental competence, the insoluble fraction or its part is necessary. The soluble fraction of GV is sufficient for physical parts of the sperm head, while the insoluble fraction is critical

for the paternal genome function. This was also another reason why it would be interesting to test the role of lamin A/C in active demethylation.

For this reason, the first step of the experiment was determination of the amount of lamin A/C protein in one GV oocyte. The method of comparing the known protein amount was used for the determination. For this standard curve and western blot method was chosen. The serial dilution of recombinant protein lamin A/C was prepared. The putative amount was counted with computer software. Even though the measurement was done five times, it is still only an indicative amount. The amount of protein lamin A/C per one GV was determinated to be 51,45 pg.

The standard curve was prepared via serial dilution of recombinant protein. The optimization of protein concentration was important. For generation of functional standard curve, at least five bands had to be visible on the membrane. For that, the concentration could not be diluted beyond 0,512 ng/µl. At the same time, the samples with the highest concentration could not contain too much of the recombinant protein. If the recombinant protein was too concentrated, the band signal was impossible to measure in the Fiji software, because the signal emission was too strong. For that the optimal concentration was 50 ng/µl.

Unfortunately, the main experiment of the project was not carried out due to a lack of time caused by long optimization time and PCR issues. The main experiment was planned as follows: from the GV oocyte the insoluble fraction would have been removed by SE while the soluble fraction would have stayed in the GV cytoplast. Next, the appropriate volume of recombinant protein lamin A/C (this information was obtained in the second part of the project) would have been microinjected to the SE-GV oocytes. Here lamin A/C would have represented the single member of insoluble GV fraction. GV oocytes prepared like this would have been fertilized by classical IVF. The fertilized oocytes would have been cultivated prior to 8 hours post fertilization. The DNA methylation of these SE-GV derived zygotes would have been elucidated. The previously mentioned bisulfite sequencing would have been used.

Nevertheless, an alternative experiment was carried out to complete the answers. All the samples were prepared by Mgr. Helena Fulka, Ph.D. The SE-GV oocytes were replaced by enucleated MII oocytes. MII is a stage of oocyte which is ready to be fertilized and therefore it has the full competence to rebuild sperm head and reprogram paternal genome. One of the conditions for this is a high level of maturation promoting factor (MPF) in the oocyte. During GV maturation, the MPF level grows. One of the effects of high level of MPF is GVBD (H. S. Lee

et al., 2016). The GV nuclear membrane turns into a “soluble” phase, and it is spread into cytoplast. During GVBD, the chromosomes are condensed, and the oocyte enters the MII stage. Right at this moment the enucleation was performed. From the MII oocyte, chromosomes and stably bound nuclear proteins were removed while the nuclear envelope including nuclear lamina and lamin A/C remained in the cytoplast. The presence of lamin A/C in the MII cytoplast was also confirmed by western blot method (Figure 14).

MII oocytes without maternal genome and some other parts of insoluble fraction, but with the protein lamin A/C at the same time, could serve as a good compensation for SE-GV. The IVF with enucleated MII was performed. This has generated androgenetic embryos with only the paternal genome. Then the process continued as it was planned for the primary experiment. After required time for cultivation, DNA from androgenetic embryos was isolated and bisulfite sequencing was performed.

The results from the last presented part are that there was minimal demethylation in androgenetic embryos after fertilization. Compared to the SE-driven embryos, the results were identical (Figure 15). The presence of lamin A/C was not sufficient for proceeding of the DNA demethylation.

However, this study cannot completely refute the conclusion of Maynard et al. Their work was more focused on lamin A/C as an initiator of BER pathway in the indirect manner. Thus, the DNA methylation level of androgenetic embryos only points to the fact that if there is an activation of the BER pathway right after fertilization, lamin A/C is not the main participant.

Nevertheless, the idea of a quick repair mechanism involved in the active DNA demethylation does not seem to be completely out of place. Even though many studies have confirmed that TET3 oxidation takes an important part in DNA demethylation after fertilization, the depletion of TET3s still has a limited impact on the DNA demethylation of the paternal pronucleus. On the other hand, TET3s seem to be indispensable for neonatal growth (Tsukada et al., 2015). This might support the conclusion that at least two parallel mechanisms for active DNA demethylation co-exist. It should also be considered that the other mechanism of active demethylation starts before the 5mC oxidation. Parallel to the oxidation by TET3 followed by BER, another DNA repair pathway might be present. The idea of a self-repair pathway also supports the proposal that the strong DNA repair mechanism relies on the oocytes and is capable to repair its DSBs of DNA even in growing oocytes (Stringer et al., 2020).

As presented before, glycosylases TDG and MBD4 are well known for BER initiating. However, they cannot be considered in the process of demethylation after fertilization because they show weak activity on 5mC (J. K. Zhu, 2009). AID is another enzyme, which is able to induce BER. Nonetheless, AID seems to be active later, more coincidentally with first replication in zygote (Santos et al., 2013).

Also, as it was mentioned in the Literary overview, DNMT3a and DNMT3b are able to deaminate the 5mC and generate T in consequence of creation T – G mismatches. (Boland & Christman, 2008). Plus, DNMT3s are obviously present in zygotes, because it was investigated that besides the active DNA demethylation, the methylation *de novo* occurs after fertilization as well (Booth et al., 2013). Surprisingly, in special conditions DNMT1 and DNMT3 are capable of acting as DNA demethylases (Chen et al., 2013). In addition, DNMT1 acts together with MBD4 in oxidative stress response. Oxidative stress causes breaks which mostly occur at CpG islands of highly transcribed genes (Laget et al., 2014). All these together lead to the suggestion that DNMT1 and DNMT3 might be considered to offer more detail in the elucidation of the active DNA demethylation question.

In conclusion, DNA methylation belongs to epigenetic reprogramming. In the early embryo DNA methylation is a complex process promoted by dynamic mechanisms. These are not only the active DNA demethylation and Tet3-driven 5mC hydroxylation and *de novo* DNA methylation as well but also correct chromatin remodelling, paternal protamine-to-histone exchange and other epigenetics that might have an impact to proper DNA modification necessary for proper embryo development. In this study it was confirmed that the key to the mechanism for active demethylation resides in the insoluble fraction of GV. However, protein lamin A/C was excluded as a potential starter for repair mechanism BER in direct manner, which may lead to the rapid loss of paternal methylation.

Detection of the influence of GV on the proper paternal reprogramming and its impact on the proper early embryo development would also be interesting for assisted reproductive technologies and centres of assisted reproduction. Despite the correct work of embryologists, the success ratio is not as satisfying as it would be expected (Mukhtar et al., 2017). This could be caused by any underlying process, which is hidden inside. Knowledge of the right GV component responsible for the paternal genome reprograming could be the key to saving numerous pregnancies. Maybe one of the reasons for abortions in the period of early embryonic development could be the mutations in gene for such a component.

8 Conclusion

- The DNA methylation level of Nanog and Oct-4 gene promoters in gametes and zygotes (before and after fertilization) was verified. The DNA methylation is lost actively after fertilization.
- Compared to the standard curve prepared by serial dilution the amount of protein lamin A/C per one GV oocyte was determined.
- Due to the lack of time the main experiment has not been proceeded. Fortunately, thanks to the work of Mgr. Helena Fulka, PhD. and Bc. Zuzana Smékalová, the rescue experiment was set up.
- Selectively enucleated embryos were prepared. It was demonstrated that the loss of insoluble GV fraction has a negative impact on the DNA demethylation after fertilization.
- Androgenetic embryos were prepared. The cytoplast of enucleated MII oocytes contained protein lamin A/C. It was demonstrated that the presence of protein lamin A/C has no positive impact to the DNA demethylation after fertilization.
- It was proved that the insoluble fraction of GV or some part of it is necessary for active DNA demethylation after fertilization. At the same time protein lamin A/C, a part of insoluble GV fraction, was excluded as a possible candidate in this process.

9 References

Adenot, P. G., Mercier, Y., Renard, J. P., & Thompson, E. M. (1997). Differential H4 acetylation of paternal and maternal chromatin precedes DNA replication and differential transcriptional activity in pronuclei of 1-cell mouse embryos. *Development*, *124*(22), 4615–4625. https://doi.org/10.1242/dev.124.22.4615

Al-Khtib, M., Blachère, T., Guérin, J. F., & Lefèvre, A. (2012). Methylation profile of the promoters of Nanog and Oct4 in ICSI human embryos. *Human Reproduction*, *27*(10). https://doi.org/10.1093/humrep/des284

Amouroux, R., Nashun, B., Shirane, K., Nakagawa, S., Hill, P. W. S., D'Souza, Z., Nakayama, M., Matsuda, M., Turp, A., Ndjetehe, E., Encheva, V., Kudo, N. R., Koseki, H., Sasaki, H., & Hajkova, P. (2016). De novo DNA methylation drives 5hmC accumulation in mouse zygotes. *Nature Cell Biology*, *18*(2). https://doi.org/10.1038/ncb3296

Bhattacharya, S. K., Ramchandani, S., Cervoni, N., & Szyf, M. (1999). A mammalian protein with specific demethylase activity for mCpG DNA. *Nature*, *397*(6720). https://doi.org/10.1038/17533

Bhutani, N., Brady, J. J., Damian, M., Sacco, A., Corbel, S. Y., & Blau, H. M. (2010). Reprogramming towards pluripotency requires AID-dependent DNA demethylation. *Nature*, *463*(7284). https://doi.org/10.1038/nature08752

Bochtler, M., Kolano, A., & Xu, G. L. (2017). DNA demethylation pathways: Additional players and regulators. *BioEssays*, *39*(1), 1–13. https://doi.org/10.1002/bies.201600178

Boland, M. J., & Christman, J. K. (2008). Characterization of Dnmt3b:Thymine-DNA Glycosylase Interaction and Stimulation of Thymine Glycosylase-Mediated Repair by DNA Methyltransferase(s) and RNA. *Journal of Molecular Biology*, *379*(3). https://doi.org/10.1016/j.jmb.2008.02.049

Booth, M. J., Ost, T. W. B., Beraldi, D., Bell, N. M., Branco, M. R., Reik, W., & Balasubramanian, S. (2013). Oxidative bisulfite sequencing of 5-methylcytosine and 5-hydroxymethylcytosine. *Nature Protocols*, *8*(10). https://doi.org/10.1038/nprot.2013.115

Borsos, M., Perricone, S. M., Schauer, T., Pontabry, J., de Luca, K. L., de Vries, S. S., Ruiz-Morales, E. R., Torres-Padilla, M. E., & Kind, J. (2019). Genome–lamina interactions are established de novo in the early mouse embryo. *Nature*, *569*(7758). https://doi.org/10.1038/s41586-019-1233-0

Chen, C. C., Wang, K. Y., & Shen, C. K. J. (2013). DNA 5-methylcytosine demethylation activities of the mammalian DNA methyltransferases. *Journal of Biological Chemistry*, *288*(13). https://doi.org/10.1074/jbc.M112.445585

Choi, H. W., Joo, J. Y., Hong, Y. J., Kim, J. S., Song, H., Lee, J. W., Wu, G., Schöler, H. R., & Do, J. T. (2016). Distinct Enhancer Activity of Oct4 in Naive and Primed Mouse Pluripotency. *Stem Cell Reports*, *7*(5), 911–926. https://doi.org/10.1016/j.stemcr.2016.09.012

Chong, S., Vickaryous, N., Ashe, A., Zamudio, N., Youngson, N., Hemley, S., Stopka, T., Skoultchi, A., Matthews, J., Scott, H. S., de Kretser, D., O'Bryan, M., Blewitt, M., & Whitelaw, E. (2007). Modifiers of epigenetic reprogramming show paternal effects in the mouse. *Nature Genetics*, *39*(5). https://doi.org/10.1038/ng2031

Davies, B. S. J., Coffinier, C., Yang, S. H., Jung, H. J., Fong, L. G., & Young, S. G. (2011). Posttranslational Processing of Nuclear Lamins. In *Enzymes* (Vol. 29). https://doi.org/10.1016/B978-0-12-381339-8.00003-2

Dawlaty, M. M., Breiling, A., Le, T., Barrasa, M. I., Raddatz, G., Gao, Q., Powell, B. E., Cheng, A. W., Faull, K. F., Lyko, F., & Jaenisch, R. (2014). Loss of tet enzymes compromises proper differentiation of embryonic stem cells. *Developmental Cell*, *29*(1). https://doi.org/10.1016/j.devcel.2014.03.003

de Bont, R., & van Larebeke, N. (2004). Endogenous DNA damage in humans: A review of quantitative data. In *Mutagenesis* (Vol. 19, Issue 3). https://doi.org/10.1093/mutage/geh025

Dechat, T., Pfleghaar, K., Sengupta, K., Shimi, T., Shumaker, D. K., Solimando, L., & Goldman, R. D. (2008). Nuclear lamins: Major factors in the structural organization and function of the nucleus and chromatin. In *Genes and Development* (Vol. 22, Issue 7). https://doi.org/10.1101/gad.1652708

Dittmer, T., & Misteli, T. (2011). The lamin protein family. *Genome Biology*, *12*(5). https://doi.org/10.1186/gb-2011-12-5-222

Donkin, I., & Barrès, R. (2018). Sperm epigenetics and influence of environmental factors. In *Molecular Metabolism* (Vol. 14). https://doi.org/10.1016/j.molmet.2018.02.006

Eckersley-Maslin, M. A., Alda-Catalinas, C., & Reik, W. (2018). Dynamics of the epigenetic landscape during the maternal-to-zygotic transition. *Nature Reviews Molecular Cell Biology*, *19*(7), 436–450. https://doi.org/10.1038/s41580-018-0008-z

el Hajj, N., Zechner, U., Schneider, E., Tresch, A., Gromoll, J., Hahn, T., Schorsch, M., & Haaf, T. (2011). Methylation status of imprinted genes and repetitive elements in sperm DNA from infertile males. *Sexual Development*, *5*(2). https://doi.org/10.1159/000323806

Esadze, A., Rodriguez, G., Cravens, S. L., & Stivers, J. T. (2017). AP-Endonuclease 1 Accelerates Turnover of Human 8-Oxoguanine DNA Glycosylase by Preventing Retrograde Binding to the Abasic-Site Product. *Biochemistry*, *56*(14). https://doi.org/10.1021/acs.biochem.7b00017

Farthing, C. R., Ficz, G., Ng, R. K., Chan, C. F., Andrews, S., Dean, W., Hemberger, M., & Reik, W. (2008). Global mapping of DNA methylation in mouse promoters reveals epigenetic reprogramming of pluripotency genes. *PLoS Genetics*, *4*(6). https://doi.org/10.1371/journal.pgen.1000116

Fortini, P., & Dogliotti, E. (2007). Base damage and single-strand break repair: Mechanisms and functional significance of short- and long-patch repair subpathways. *DNA Repair*, *6*(4), 398–409. https://doi.org/10.1016/j.dnarep.2006.10.008

Frommer, M., Mcdonald, L. E., Millar, D. S., Collist, C. M., Wattt, F., Griggt, G. W., Molloyt, P. L., & Paul, C. L. (1992). *A genomic sequencing protocol that yields a positive display of 5-methylcytosine residues in individual DNA strands*. *89*(March), 1827–1831.

Gardiner-Garden, M., & Frommer, M. (1987). CpG Islands in vertebrate genomes. *Journal of Molecular Biology*, *196*(2). https://doi.org/10.1016/0022-2836(87)90689-9

Gehring, M., Reik, W., & Henikoff, S. (2009). DNA demethylation by DNA repair. *Trends in Genetics*, *25*(2), 82–90. https://doi.org/10.1016/j.tig.2008.12.001

Gilbert, S. F. (2014). Developmental Biology, 10th edition. Sinauer Associates, ISBN 978-0-87893-978-7

Godmann, M., Lambrot, R., & Kimmins, S. (2009). The dynamic epigenetic program in male germ cells: Its role in spermatogenesis, testis cancer, and its response to the environment. In *Microscopy Research and Technique* (Vol. 72, Issue 8). https://doi.org/10.1002/jemt.20715

Gong, Z., & Zhu, J. K. (2011). Active DNA demethylation by oxidation and repair. *Cell Research*, *21*(12). https://doi.org/10.1038/cr.2011.140

Gu, T. P., Guo, F., Yang, H., Wu, H. P., Xu, G. F., Liu, W., Xie, Z. G., Shi, L., He, X., Jin, S. G., Iqbal, K., Shi, Y. G., Deng, Z., Szabó, P. E., Pfeifer, G. P., Li, J., & Xu, G. L. (2011). The role of Tet3 DNA dioxygenase in epigenetic reprogramming by oocytes. *Nature*, *477*(7366). https://doi.org/10.1038/nature10443

Guelen, L., Pagie, L., Brasset, E., Meuleman, W., Faza, M. B., Talhout, W., Eussen, B. H., de Klein, A., Wessels, L., de Laat, W., & van Steensel, B. (2008). Domain organization of human chromosomes revealed by mapping of nuclear lamina interactions. *Nature*, *453*(7197). https://doi.org/10.1038/nature06947

Guibert, S., Forné, T., & Weber, M. (2012). Global profiling of DNA methylation erasure in mouse primordial germ cells. *Genome Research*, *22*(4). https://doi.org/10.1101/gr.130997.111

Guo, F., Li, X., Liang, D., Li, T., Zhu, P., Guo, H., Wu, X., Wen, L., Gu, T. P., Hu, B., Walsh, C. P., Li, J., Tang, F., & Xu, G. L. (2014). Active and passive demethylation of male and female pronuclear DNA in the mammalian zygote. *Cell Stem Cell*, *15*(4). https://doi.org/10.1016/j.stem.2014.08.003

Hackett, J. A., Sengupta, R., Zylicz, J. J., Murakami, K., Lee, C., Down, T. A., & Surani, M. A. (2013). Germline DNA demethylation dynamics and imprint erasure through 5-hydroxymethylcytosine. *Science*, *339*(6118). https://doi.org/10.1126/science.1229277

Hajkova, P., Erhardt, S., Lane, N., Haaf, T., El-Maarri, O., Reik, W., Walter, J., & Surani, M. A. (2002). Epigenetic reprogramming in mouse primordial germ cells. *Mechanisms of Development*, *117*(1–2). https://doi.org/10.1016/S0925-4773(02)00181-8

Hajkova, P., Jeffries, S. J., Lee, C., Miller, N., Jackson, S. P., & Surani, M. A. (2010). Genome-wide reprogramming in the mouse germ line entails the base excision repair pathway. *Science*, *329*(5987), 78–82. https://doi.org/10.1126/science.1187945

Hatanaka, Y., Shimizu, N., Nishikawa, S., Tokoro, M., Shin, S. W., Nishihara, T., Amano, T., Anzai, M., Kato, H., Mitani, T., Hosoi, Y., Kishigami, S., & Matsumoto, K. (2013). GSE Is a Maternal Factor Involved in Active DNA Demethylation in Zygotes. *PLoS ONE*, *8*(4). https://doi.org/10.1371/journal.pone.0060205

He, Y. F., Li, B. Z., Li, Z., Liu, P., Wang, Y., Tang, Q., Ding, J., Jia, Y., Chen, Z., Li, N., Sun, Y., Li, X., Dai, Q., Song, C. X., Zhang, K., He, C., & Xu, G. L. (2011). Tet-mediated formation of 5-carboxylcytosine and its excision by TDG in mammalian DNA. *Science*, *333*(6047). https://doi.org/10.1126/science.1210944

Hendrich, B., Hardeland, U., Ng, H. H., Jiricny, J., & Bird, A. (1999). The thymine glycosylase MBD4 can bind to the product of deamination at methylated CpG sites. *Nature*, *401*(6750). https://doi.org/10.1038/45843

Hermann, A., Goyal, R., & Jeltsch, A. (2004). The Dnmt1 DNA-(cytosine-C5)-methyltransferase methylates DNA processively with high preference for hemimethylated target sites. *Journal of Biological Chemistry*, *279*(46). https://doi.org/10.1074/jbc.M403427200

Houliston, E., Guilly, M. N., Courvalin, J. C., & Maro, B. (1988). Expression of nuclear lamins during mouse preimplantation development. *Development*, *102*(2). https://doi.org/10.1242/dev.102.2.271

Ichiyanagi, T., Ichiyanagi, K., Miyake, M., & Sasaki, H. (2013). Accumulation and loss of asymmetric non-CpG methylation during male germ-cell development. *Nucleic Acids Research*, *41*(2). https://doi.org/10.1093/nar/gks1117

Inoue, A., Shen, L., Dai, Q., He, C., & Zhang, Y. (2011). Generation and replication-dependent dilution of 5fC and 5caC during mouse preimplantation development. *Cell Research*, *21*(12). https://doi.org/10.1038/cr.2011.189

Iqbal, K., Jin, S. G., Pfeifer, G. P., & Szabó, P. E. (2011). Reprogramming of the paternal genome upon fertilization involves genome-wide oxidation of 5-methylcytosine. *Proceedings of the National Academy of Sciences of the United States of America*, *108*(9). https://doi.org/10.1073/pnas.1014033108

Ito, S., Shen, L., Dai, Q., Wu, S. C., Collins, L. B., Swenberg, J. A., He, C., & Zhang, Y. (2011). Tet proteins can convert 5-methylcytosine to 5-formylcytosine and 5-carboxylcytosine. *Science*, *333*(6047). https://doi.org/10.1126/science.1210597

Iurlaro, M., von Meyenn, F., & Reik, W. (2017). DNA methylation homeostasis in human and mouse development. In *Current Opinion in Genetics and Development* (Vol. 43). https://doi.org/10.1016/j.gde.2017.02.003

Iyer, L. M., Tahiliani, M., Rao, A., & Aravind, L. (2009). Prediction of novel families of enzymes involved in oxidative and other complex modifications of bases in nucleic acids. *Cell Cycle*, *8*(11). https://doi.org/10.4161/cc.8.11.8580

Iyer, L. M., Zhang, D., & Aravind, L. (2016). Adenine methylation in eukaryotes: Apprehending the complex evolutionary history and functional potential of an epigenetic modification. *BioEssays*, *38*(1). https://doi.org/10.1002/bies.201500104

Jacobs, A. L., & Schär, P. (2012). DNA glycosylases: In DNA repair and beyond. In *Chromosoma* (Vol. 121, Issue 1). https://doi.org/10.1007/s00412-011-0347-4

Kaneda, M., Okano, M., Hata, K., Sado, T., Tsujimoto, H., Li, E., & Sasaki, H. (2004). Essential role for de novo DNA methyltransferase Dnmt3a in paternal and maternal imprinting. *Nature*, *429*(6994). https://doi.org/10.1038/nature02633

Kanvah, S., Joseph, J., Schuster, G. B., Barnett, R. N., Cleveland, C. L., & Landman, U. Z. I. (2010). Oxidation of DNA: Damage to nucleobases. *Accounts of Chemical Research*, *43*(2). https://doi.org/10.1021/ar900175a

Kim, K. H., Kim, E. Y., Lee, S. Y., Ko, J. J., & Lee, K. A. (2018). Oocyte Cytoplasmic Gas6 and Heparan Sulfate (HS) are Required to Establish the Open Chromatin State in Nuclei during Remodeling and Reprogramming. *Cellular Physiology and Biochemistry*, *45*(1). https://doi.org/10.1159/000486221

Kim, S. H., Kang, Y. K., Koo, D. B., Kang, M. J., Moon, S. J., Lee, K. K., & Han, Y. M. (2004). Differential DNA methylation reprogramming of various repetitive sequences in mouse preimplantation embryos. *Biochemical and Biophysical Research Communications*, *324*(1). https://doi.org/10.1016/j.bbrc.2004.09.023

Kobayashi, H., Sakurai, T., Imai, M., Takahashi, N., Fukuda, A., Yayoi, O., Sato, S., Nakabayashi, K., Hata, K., Sotomaru, Y., Suzuki, Y., & Kono, T. (2012). Contribution of intragenic DNA

methylation in mouse gametic DNA methylomes to establish Oocyte-specific heritable marks. *PLoS Genetics*, *8*(1). https://doi.org/10.1371/journal.pgen.1002440

Kobayashi, H., Sakurai, T., Miura, F., Imai, M., Mochiduki, K., Yanagisawa, E., Sakashita, A., Wakai, T., Suzuki, Y., Ito, T., Matsui, Y., & Kono, T. (2013). High-resolution DNA methylome analysis of primordial germ cells identifies gender-specific reprogramming in mice. *Genome Research*, *23*(4). https://doi.org/10.1101/gr.148023.112

Kohda, T., & Ishino, F. (2013). Embryo manipulation via assisted reproductive technology and epigenetic asymmetry in mammalian early development. *Philosophical Transactions of the Royal Society B: Biological Sciences*, *368*(1609). https://doi.org/10.1098/rstb.2012.0353

Laget, S., Miotto, B., Chin, H. G., Estève, P. O., Roberts, R. J., Pradhan, S., & Defossez, P. A. (2014). MBD4 cooperates with DNMT1 to mediate methyl-DNA repression and protects mammalian cells from oxidative stress. *Epigenetics*, *9*(4). https://doi.org/10.4161/epi.27695

Lammerding, J., Fong, L. G., Ji, J. Y., Reue, K., Stewart, C. L., Young, S. G., & Lee, R. T. (2006). Lamins a and C but not lamin B1 regulate nuclear mechanics. *Journal of Biological Chemistry*, *281*(35). https://doi.org/10.1074/jbc.M513511200

Lane, N., Dean, W., Erhardt, S., Hajkova, P., Surani, A., Walter, J., & Reik, W. (2003). Resistance of IAPs to methylation reprogramming may provide a mechanism for epigenetic inheritance in the mouse. *Genesis*, *35*(2), 88–93. https://doi.org/10.1002/gene.10168

Lee, H. S., Kim, K. H., Kim, E. Y., Lee, S. Y., Ko, J. J., & Lee, K. A. (2016). Obox4-silencing-activated STAT3 and MPF/MAPK signaling accelerate nuclear membrane breakdown in mouse oocytes. *Reproduction*, *151*(4). https://doi.org/10.1530/REP-15-0020

Lee, T. H., & Kang, T. H. (2019). DNA oxidation and excision repair pathways. *International Journal of Molecular Sciences*, *20*(23). https://doi.org/10.3390/ijms20236092

Lio, C. W. J., Yue, X., López-Moyado, I. F., Tahiliani, M., Aravind, L., & Rao, A. (2020). TET methylcytosine oxidases: new insights from a decade of research. In *Journal of Biosciences* (Vol. 45, Issue 1). Springer. https://doi.org/10.1007/s12038-019-9973-4

Luberda, Z. (2005). The role of glutathione in mammalian gametes. In *Reproductive biology* (Vol. 5, Issue 1).

Ma, D. K., Jang, M. H., Guo, J. U., Kitabatake, Y., Chang, M. L., Pow-anpongkul, N., Flavell, R. A., Lu, B., Ming, G. L., & Song, H. (2009). Neuronal activity-induced Gadd45b promotes epigenetic DNA demethylation and adult neurogenesis. *Science*, *323*(5917). https://doi.org/10.1126/science.1166859

Ma, J. Y., Zhang, T., Shen, W., Schatten, H., & Sun, Q. Y. (2014). Molecules and mechanisms controlling the active DNA demethylation of the mammalian zygotic genome. In *Protein and Cell* (Vol. 5, Issue 11). https://doi.org/10.1007/s13238-014-0095-3

Maiti, A., & Drohat, A. C. (2011). Thymine DNA glycosylase can rapidly excise 5-formylcytosine and 5-carboxylcytosine: Potential implications for active demethylation of CpG sites. *Journal of Biological Chemistry*, *286*(41). https://doi.org/10.1074/jbc.C111.284620

Marques, C. J., Francisco, T., Sousa, S., Carvalho, F., Barros, A., & Sousa, M. (2010). Methylation defects of imprinted genes in human testicular spermatozoa. *Fertility and Sterility*, *94*(2). https://doi.org/10.1016/j.fertnstert.2009.02.051

Martin, J. L., & McMillan, F. M. (2002). SAM (dependent) I AM: The S-adenosylmethionine-dependent methyltransferase fold. In *Current Opinion in Structural Biology* (Vol. 12, Issue 6). https://doi.org/10.1016/S0959-440X(02)00391-3

Matoba, S., & Zhang, Y. (2018). Somatic Cell Nuclear Transfer Reprogramming: Mechanisms and Applications. In *Cell Stem Cell* (Vol. 23, Issue 4). https://doi.org/10.1016/j.stem.2018.06.018

Maynard, S., Keijzers, G., Akbari, M., Ezra, M. ben, Hall, A., Morevati, M., Scheibye-Knudsen, M., Gonzalo, S., Bartek, J., & Bohr, V. A. (2019). Lamin A/C promotes DNA base excision repair. *Nucleic Acids Research*, *47*(22), 11709–11728. https://doi.org/10.1093/nar/gkz912

McLay, D. W., & Clarke, H. J. (2003). Remodelling the paternal chromatin at fertilization in mammals. In *Reproduction* (Vol. 125, Issue 5). https://doi.org/10.1530/rep.0.1250625

Merriam, R. W., & Hill, R. J. (1976). The germinal vesicle nucleus of Xenopus Laevis oocytes as a selective storage receptacle for proteins. *Journal of Cell Biology*, *69*(3). https://doi.org/10.1083/jcb.69.3.659

Messerschmidt, D. M., Knowles, B. B., & Solter, D. (2014). DNA methylation dynamics during epigenetic reprogramming in the germline and preimplantation embryos. In *Genes and Development* (Vol. 28, Issue 8). https://doi.org/10.1101/gad.234294.113

Mizuno, S., Sono, Y., Matsuoka, T., Matsumoto, K., Saeki, K., Hosoi, Y., Fukuda, A., Morimoto, Y., & Iritani, A. (2006). Expression and subcellular localization of GSE protein in germ cells and preimplantation embryos. *Journal of Reproduction and Development*, *52*(3). https://doi.org/10.1262/jrd.18005

Moore, L. D., Le, T., & Fan, G. (2013). DNA methylation and its basic function. In *Neuropsychopharmacology* (Vol. 38, Issue 1). https://doi.org/10.1038/npp.2012.112

Morgan, H. D., Dean, W., Coker, H. A., Reik, W., & Petersen-Mahrt, S. K. (2004). Activation-induced cytidine deaminase deaminates 5-methylcytosine in DNA and is expressed in pluripotent tissues: Implications for epigenetic reprogramming. *Journal of Biological Chemistry*, *279*(50). https://doi.org/10.1074/jbc.M407695200

Mukhtar, H. B., Shaman, A., Mirghani, H. O., & Almasalmah, A. A. (2017). The outcome of assisted reproductive techniques among couples with male factors at prince khalid bin sultan fertility centre, Kingdom of Saudi Arabia. *Open Access Macedonian Journal of Medical Sciences*, *5*(5). https://doi.org/10.3889/oamjms.2017.102

Nakamura, T., Arai, Y., Umehara, H., Masuhara, M., Kimura, T., Taniguchi, H., Sekimoto, T., Ikawa, M., Yoneda, Y., Okabe, M., Tanaka, S., Shiota, K., & Nakano, T. (2007). PGC7/Stella protects against DNA demethylation in early embryogenesis. *Nature Cell Biology*, *9*(1). https://doi.org/10.1038/ncb1519

Neddermann, P., Gallinari, P., Lettieri, T., Schmid, D., Truong, O., Hsuan, J. J., Wiebauer, K., & Jiricny, J. (1996). Cloning and expression of human G/T mismatch-specific thymine-DNA

glycosylase. *Journal of Biological Chemistry*, *271*(22). https://doi.org/10.1074/jbc.271.22.12767

Niforou, K. N., Anagnostopoulos, A. K., Vougas, K., Kittas, C., Gorgoulis, V. G., & Tsangaris, G. T. (2008). The proteome profile of the human osteosarcoma U2OS cell line. *Cancer Genomics and Proteomics*, *5*(1).

Ogushi, S., Fulka, J., & Miyano, T. (2005). Germinal vesicle materials are requisite for male pronucleus formation but not for change in the activities of CDK1 and MAP kinase during maturation and fertilization of pig oocytes. *Developmental Biology*, *286*(1), 287–298. https://doi.org/10.1016/j.ydbio.2005.08.002

Okano, M., Bell, D. W., Haber, D. A., & Li, E. (1999). DNA methyltransferases Dnmt3a and Dnmt3b are essential for de novo methylation and mammalian development. *Cell*, *99*(3). https://doi.org/10.1016/S0092-8674(00)81656-6

Pappas, J. J., Toulouse, A., & Bradley, W. E. C. (2013). The bisulfite genomic sequencing protocol. *Advances in Lung Cancer*, *02*(01), 21–25. https://doi.org/10.4236/alc.2013.21004

Peric-Hupkes, D., Meuleman, W., Pagie, L., Bruggeman, S. W. M., Solovei, I., Brugman, W., Gräf, S., Flicek, P., Kerkhoven, R. M., van Lohuizen, M., Reinders, M., Wessels, L., & van Steensel, B. (2010). Molecular Maps of the Reorganization of Genome-Nuclear Lamina Interactions during Differentiation. *Molecular Cell*, *38*(4). https://doi.org/10.1016/j.molcel.2010.03.016

Perreault, S. D. (1992). Chromatin remodeling in mammalian zygotes. *Mutation Research/Reviews in Genetic Toxicology*, *296*(1–2). https://doi.org/10.1016/0165-1110(92)90031-4

Rai, K., Huggins, I. J., James, S. R., Karpf, A. R., Jones, D. A., & Cairns, B. R. (2008). DNA Demethylation in Zebrafish Involves the Coupling of a Deaminase, a Glycosylase, and Gadd45. *Cell*, *135*(7). https://doi.org/10.1016/j.cell.2008.11.042

Ramchandani, S., Bhattacharya, S. K., Cervoni, N., & Szyf, M. (1999). DNA methylation is a reversible biological signal. *Proceedings of the National Academy of Sciences of the United States of America*, *96*(11). https://doi.org/10.1073/pnas.96.11.6107

Rankin, J., & Ellard, S. (2006). The laminopathies: A clinical review. In *Clinical Genetics* (Vol. 70, Issue 4). https://doi.org/10.1111/j.1399-0004.2006.00677.x

Ratnam, S., Mertineit, C., Ding, F., Howell, C. Y., Clarke, H. J., Bestor, T. H., Chaillet, J. R., & Trasler, J. M. (2002). Dynamics of Dnmt1 methyltransferase expression and intracellular localization during oogenesis and preimplantation development. *Developmental Biology*, *245*(2). https://doi.org/10.1006/dbio.2002.0628

Redwood, A. B., Gonzalez-suarez, I., & Gonzalo, S. (2011). Regulating the levels of key factors in cell cycle and DNA repair. *Cell Cycle*, *10*(21), 3652–3657.

Rober, R.-A., Weber, K., & Osborn, M. (1989). Differential timing of nuclear lamin A/C expression in the various organs of the mouse embryo and the young animal: a developmental study. *Development*, *105*, 365–378.

Robertson, A. B., Klungland, A., Rognes, T., & Leiros, I. (2009). Base excision repair: The long and short of it. In *Cellular and Molecular Life Sciences* (Vol. 66, Issue 6). https://doi.org/10.1007/s00018-009-8736-z

Romanato, M., Julianelli, V., Zappi, M., Calvo, L., & Calvo, J. C. (2008). The presence of heparan sulfate in the mammalian oocyte provides a clue to human sperm nuclear decondensation in vivo. *Human Reproduction*, *23*(5). https://doi.org/10.1093/humrep/den028

Rougier, N., Bourc'his, D., Molina Gomes, D., Niveleau, A., Plachot, M., Pàldi, A., & Viegas-Péquignot, E. (1998). Chromosome methylation patterns during mammalian preimplantation development. *Genes and Development*, *12*(14). https://doi.org/10.1101/gad.12.14.2108

Saga, Y. (2008). Mouse germ cell development during embryogenesis. In *Current Opinion in Genetics and Development* (Vol. 18, Issue 4). https://doi.org/10.1016/j.gde.2008.06.003

Sakai, Y., Suetake, I., Shinozaki, F., Yamashina, S., & Tajima, S. (2004). Co-expression of de novo DNA methyltransferases Dnmt3a2 and Dnmt3L in gonocytes of mouse embryos. *Gene Expression Patterns*, *5*(2). https://doi.org/10.1016/j.modgep.2004.07.011

Santos, F., Hendrich, B., Reik, W., & Dean, W. (2002). Dynamic reprogramming of DNA methylation in the early mouse embryo. *Developmental Biology*, *241*(1), 172–182. https://doi.org/10.1006/dbio.2001.0501

Santos, F., Peat, J., Burgess, H., Rada, C., Reik, W., & Dean, W. (2013). Active demethylation in mouse zygotes involves cytosine deamination and base excision repair. *Epigenetics and Chromatin*, *6*(1). https://doi.org/10.1186/1756-8935-6-39

Schuermann, D., Weber, A. R., & Schär, P. (2016). Active DNA demethylation by DNA repair: Facts and uncertainties. *DNA Repair*, *44*, 92–102. https://doi.org/10.1016/j.dnarep.2016.05.013

Seisenberger, S., Peat, J. R., Hore, T. A., Santos, F., Dean, W., & Reik, W. (2013). Reprogramming DNA methylation in the mammalian life cycle: Building and breaking epigenetic barriers. *Philosophical Transactions of the Royal Society B: Biological Sciences*, *368*(1609), 1–11. https://doi.org/10.1098/rstb.2011.0330

Shen, L., Inoue, A., He, J., Liu, Y., Lu, F., & Zhang, Y. (2014). Tet3 and DNA replication mediate demethylation of both the maternal and paternal genomes in mouse zygotes. *Cell Stem Cell*, *15*(4). https://doi.org/10.1016/j.stem.2014.09.002

Shen, L., Wu, H., Diep, D., Yamaguchi, S., D'Alessio, A. C., Fung, H. L., Zhang, K., & Zhang, Y. (2013). Genome-wide analysis reveals TET- and TDG-dependent 5-methylcytosine oxidation dynamics. *Cell*, *153*(3). https://doi.org/10.1016/j.cell.2013.04.002

Smallwood, S. A., Tomizawa, S. I., Krueger, F., Ruf, N., Carli, N., Segonds-Pichon, A., Sato, S., Hata, K., Andrews, S. R., & Kelsey, G. (2011). Dynamic CpG island methylation landscape in oocytes and preimplantation embryos. *Nature Genetics*, *43*(8). https://doi.org/10.1038/ng.864

Stewart, C., & Burke, B. (1987). Teratocarcinoma stem cells and early mouse embryos contain only a single major lamin polypeptide closely resembling lamin B. *Cell*, *51*(3). https://doi.org/10.1016/0092-8674(87)90634-9

Stringer, J. M., Winship, A., Zerafa, N., Wakefield, M., & Hutt, K. (2020). Oocytes can efficiently repair DNA double-strand breaks to restore genetic integrity and protect offspring health. *Proceedings of the National Academy of Sciences of the United States of America*, *117*(21). https://doi.org/10.1073/pnas.2001124117

Suzuki, M. M., & Bird, A. (2008). DNA methylation landscapes: Provocative insights from epigenomics. In *Nature Reviews Genetics* (Vol. 9, Issue 6). https://doi.org/10.1038/nrg2341

Tahiliani, M., Koh, K. P., Shen, Y., Pastor, W. A., Bandukwala, H., Brudno, Y., Agarwal, S., Iyer, L. M., Liu, D. R., Aravind, L., & Rao, A. (2009). Conversion of 5-methylcytosine to 5-hydroxymethylcytosine in mammalian DNA by MLL partner TET1. *Science*, *324*(5929). https://doi.org/10.1126/science.1170116

Takeo, T., & Nakagata, N. (2011). Reduced glutathione enhances fertility of frozen/thawed C57BL/6 mouse sperm after exposure to methyl-beta-cyclodextrin. *Biology of Reproduction*, *85*(5). https://doi.org/10.1095/biolreprod.111.092536

Tsai, C. C., Su, P. F., Huang, Y. F., Yew, T. L., & Hung, S. C. (2012). Oct4 and Nanog Directly Regulate Dnmt1 to Maintain Self-Renewal and Undifferentiated State in Mesenchymal Stem Cells. *Molecular Cell*, *47*(2). https://doi.org/10.1016/j.molcel.2012.06.020

Tsukada, Y. I., Akiyama, T., & Nakayama, K. I. (2015). Maternal TET3 is dispensable for embryonic development but is required for neonatal growth. *Scientific Reports*, *5*. https://doi.org/10.1038/srep15876

Tucci, V., Isles, A. R., Kelsey, G., Ferguson-Smith, A. C., Bartolomei, M. S., Benvenisty, N., Bourc'his, D., Charalambous, M., Dulac, C., Feil, R., Glaser, J., Huelsmann, L., John, R. M., McNamara, G. I., Moorwood, K., Muscatelli, F., Sasaki, H., Strassmann, B. I., Vincenz, C., & Wilkins, J. (2019). Genomic Imprinting and Physiological Processes in Mammals. In *Cell* (Vol. 176, Issue 5). https://doi.org/10.1016/j.cell.2019.01.043

Usui, N., & Yanagimachi, R. (1976). Behavior of hamster sperm nuclei incorporated into eggs at various stages of maturation, fertilization, and early development. The appearance and disappearance of factors involved in sperm chromatin decondensation in egg cytoplasm. *Journal of Ultrasructure Research*, *57*(3). https://doi.org/10.1016/S0022-5320(76)80117-7

Vazquez, B. N., Thackray, J. K., Simonet, N. G., Chahar, S., Kane-Goldsmith, N., Newkirk, S. J., Lee, S., Xing, J., Verzi, M. P., An, W., Vaquero, A., Tischfield, J. A., & Serrano, L. (2019). SIRT7 mediates L1 elements transcriptional repression and their association with the nuclear lamina. *Nucleic Acids Research*, *47*(15), 7870–7885. https://doi.org/10.1093/nar/gkz519

Vergnes, L., Péterfy, M., Bergo, M. O., Young, S. G., & Reue, K. (2004). Lamin B1 is required for mouse development and nuclear integrity. *Proceedings of the National Academy of Sciences of the United States of America*, *101*(28). https://doi.org/10.1073/pnas.0401424101

Wang, K., Chen, Y., Chang, E. A., Knott, J. G., & Cibelli, J. B. (2009). Dynamic epigenetic regulation of the oct4 and nanog regulatory regions during neural differentiation in rhesus

nuclear transfer embryonic stem cells. *Cloning and Stem Cells*, *11*(4). https://doi.org/10.1089/clo.2009.0019

Weber, M., Hellmann, I., Stadler, M. B., Ramos, L., Pääbo, S., Rebhan, M., & Schübeler, D. (2007). Distribution, silencing potential and evolutionary impact of promoter DNA methylation in the human genome. *Nature Genetics*, *39*(4). https://doi.org/10.1038/ng1990

Worman, H. J. (2012). Nuclear lamins and laminopathies HHS Public Access. *J Pathol*, *226*(2), 316–325. https://doi.org/10.1002/path.2999

Worman, H. J., Ostlund, C., & Wang, Y. (2010). Diseases of the nuclear envelope. *Cold Spring Harbor Perspectives in Biology*, *2*(2), 1–17. https://doi.org/10.1101/cshperspect.a000760

Wossidlo, M., Arand, J., Sebastiano, V., Lepikhov, K., Boiani, M., Reinhardt, R., Schöler, H., & Walter, J. (2010). Dynamic link of DNA demethylation, DNA strand breaks and repair in mouse zygotes. *EMBO Journal*, *29*(11), 1877–1888. https://doi.org/10.1038/emboj.2010.80

Wu, G., & Schöler, H. R. (2014). Role of Oct4 in the early embryo development. In *Cell Regeneration* (Vol. 3, Issue 1). https://doi.org/10.1186/2045-9769-3-7

Wu, H., de Gannes, M. K., Luchetti, G., & Richard Pilsner, J. (2015). Rapid method for the isolation of mammalian sperm DNA. *BioTechniques*, *58*(6), 293–300. https://doi.org/10.2144/000114280

Wu, S. C., & Zhang, Y. (2010). Active DNA demethylation: Many roads lead to Rome. In *Nature Reviews Molecular Cell Biology* (Vol. 11, Issue 9). https://doi.org/10.1038/nrm2950

Xu, G. L., & Walsh, C. P. (2014). Enzymatic DNA oxidation: Mechanisms and biological significance. In *BMB Reports* (Vol. 47, Issue 11). https://doi.org/10.5483/BMBRep.2014.47.11.223

Xu, J. (2005). Preparation, Culture, and Immortalization of Mouse Embryonic Fibroblasts. In *Current Protocols in Molecular Biology*. https://doi.org/10.1002/0471142727.mb2801s70

Yabuki, M., Miyake, T., Doi, Y., Fujiwara, T., Hamazaki, K., Yoshioka, T., Horton, A. A., & Utsumi, K. (1999). Role of Nuclear Lamins in Nuclear Segmentation of Human Neutrophils. *Physiological Chemistry and Physics and Medical NMR*, *31*(2).

Zhao, M. T., Rivera, R. M., & Prather, R. S. (2013). Locus-specific DNA methylation reprogramming during early porcine embryogenesis. *Biology of Reproduction*, *88*(2). https://doi.org/10.1095/biolreprod.112.104471

Zhu, C., Gao, Y., Guo, H., Xia, B., Song, J., Wu, X., Zeng, H., Kee, K., Tang, F., & Yi, C. (2017). Single-Cell 5-Formylcytosine Landscapes of Mammalian Early Embryos and ESCs at Single-Base Resolution. *Cell Stem Cell*, *20*(5). https://doi.org/10.1016/j.stem.2017.02.013

Zhu, J. K. (2009). Active DNA demethylation mediated by DNA glycosylases. In *Annual Review of Genetics* (Vol. 43). https://doi.org/10.1146/annurev-genet-102108-134205

Zuccotti, M., & Monk, M. (1995). Methylation of the mouse Xist gene in sperm and eggs correlates with imprinted Xist expression and paternal X–inactivation. *Nature Genetics*, *9*(3), 316–320. https://doi.org/10.1038/ng0395-316